



## Multi-Year ACSM measurements at the Central European Research Station Melpitz (Germany) Part I: Instrument Robustness, Quality Assurance, and Impact of Upper Size Cut-Off Diameter

5 Laurent Poulain<sup>1</sup>, Gerald Spindler<sup>1</sup>, Achim Grüner<sup>1</sup>, Thomas Tuch<sup>1</sup>, Bastian Stieger<sup>1</sup>, Dominik van Pinxteren, Hartmut Herrmann<sup>1</sup>, and Alfred Wiedensohler<sup>1</sup>

<sup>1</sup> Leibniz Institute for Tropospheric Research (TROPOS), Permoserstr. 15, 04317 Leipzig, Germany

Correspondence to: L. Poulain (poulain@tropos.de)

10

**Abstract.** The Aerosol Chemical Speciation Monitor (ACSM) is an instrument for identifying and quantifying the influence of air quality mitigations. For this purpose, a European ACSM network has been developed within the research infrastructure project ACTRIS (European Research Infrastructure for the observation of Aerosol, Clouds and Trace Gases). To ensure the uniformity of the dataset, as well as instrumental performance and variability, regular intercomparisons are organized at the  
15 Aerosol Chemical Monitoring Calibration Center (ACMCC, part of the European Center for Aerosol Calibration, Paris, France). However, in-situ quality assurance remains a fundamental tracking point of the instrument's stability. In order to check the robustness of the ACSM over the years and to characterize the seasonality effect, nitrate, sulfate, ammonium, organic, and particle mass concentrations were systematically compared with collocated measurements including daily off-line high-volume PM<sub>1</sub> and PM<sub>2.5</sub> filter samples. Mass closure analysis was made by comparing the total particle mass (PM) concentration  
20 obtained by adding the mass concentration of equivalent black carbon (eBC) from the Multi-Angle Absorption Photometer (MAAP) to the ACSM chemical composition, to that of PM<sub>1</sub> and PM<sub>2.5</sub> during filter weighting, as well as to the derived mass concentration of particle number size distribution measurements (PNSD). A combination of PM<sub>1</sub> and PM<sub>2.5</sub> filter samples helps identify the critical importance of the upper size cut-off of the ACSM during such exercises. The ACSM-MAAP-derived mass concentrations systematically deviate from the PM<sub>1</sub> samples when the mass concentration of the latter represents less than  
25 60 % of PM<sub>2.5</sub>, which is linked to the transmission efficiency of the aerodynamic lenses of the ACSM. The best correlations are obtained for sulfate (slope 0.96,  $R^2 = 0.77$ ) and total PM (slope 1.02,  $R^2 = 0.90$ ). Although, sulfate does not exhibit a seasonal dependency, total PM mass concentration shows a small seasonal effect associated with an increase in non-water-soluble fractions. The nitrate suffers from a loss of ammonium nitrate during filter collection, and the contribution of organo-nitrate compounds to the ACSM nitrate signal make it difficult to directly compare the two methods. The contribution of m/z  
30 44 ( $f_{44}$ ) to the total organic mass concentration was used to convert the ACSM organic mass to OC by using a similar approach as for the AMS. The resulting estimated OC<sub>ACSM</sub> was compared with the measured OC<sub>PM1</sub> (slope 0.74,  $R^2 = 0.77$ ), indicating



that the  $f_{44}$  signal was relatively free of interferences during this period. The  $PM_{2.5}$  filter samples use for the ACSM data quality might suffer from a systematic bias due to a size cutting effect as well as to the presence of chemical species that cannot be detected by the ACSM in coarse mode (e.g. sodium nitrate and sodium sulfate). This may lead to a systematic underestimation of the ACSM particle mass concentration and/or a positive artefact that artificially decreases the discrepancies between the two methods. Consequently, ACSM data validation using  $PM_{2.5}$  filters has to be interpreted with extreme care. The particle mass closure with the PNSD was satisfying (slope 0.77,  $R^2 = 0.90$  over the entire period), with a slightly overestimation of the MPSS-derived mass concentration in winter. This seasonal variability was related to a change on the PNSD and a larger contribution of the super- $\mu m$  particles in winter.

This long-term analysis between the ACSM and other collocated instruments confirms the robustness of the ACSM and its suitability for long-term measurements. Particle mass closure with the PNSD is strongly recommended to ensure the stability of the ACSM. A near real-time mass closure procedure within the entire ACTRIS-ACSM network certainly represents an optimal way of both warranting the quality assurance of the ACSM measurements as well as identifying possible deviations in one of the two instruments.

## 1. Introduction

Aerosol particles strongly influence our environment, having especially an impact on the ecosystem and human health. In particular, fine particulate pollution directly affects mortality and morbidity (e.g. Gurjar et al., 2010; Ostro et al., 2007). Lelieveld et al. (2015) have estimated that air pollution, mostly  $< 2.5 \mu m$  aerosol particles, may lead to 3.5 million premature deaths per year worldwide. Consequently, improving air quality represents a clear challenge, especially in urban areas. Quantifying the impact of the regulations to the air quality and changes on aerosol chemical composition needs to perform continuous and long-term measurements of aerosol particle properties such as e.g. the particle number size distribution (PNSD) and the chemical composition. For this purpose, a European network of ground-based Aerosol Chemical Species Monitor (ACSM, Ng et al., 2011) is operated within the European Research Infrastructure ACTRIS (European Research Infrastructure for the observation of Aerosol, Clouds and Trace Gases, <http://www.actris.eu>). One of the main objectives of this coordinated ACSM network is to investigate and understand the spatial variability of aerosol chemical compositions on a continental scale, including temporal variability over days, seasons, and years. With such instrumental network, it is essential to keep a strong focus on the data quality as well as to assure that the results provided by each instrument are comparable to each other. Therefore, ACSM intercomparison workshops are regularly conducted within the framework of the European Center for Aerosol Calibration (ECAC, [www.actris-ecac.eu](http://www.actris-ecac.eu)) at the Aerosol Chemical Monitor Calibration Center (ACMCC) in France. Data quality is ensured by determining instrumental variability between ACSMs (total mass 9 %, organic 19 %, nitrate 15 %, sulfate 28 %, ammonium 36 %, Crenn et al., 2015; Fröhlich et al., 2015a; Freney et al., 2019).



Although intercomparison exercises provide instrumental variability, a comparison between ACSM and collocated measurements remains a fundamental aspect of in-situ quality control. These intercomparisons are considered in a number of publications (e.g. Fröhlich et al., 2015b; Petit et al., 2015; Parworth et al., 2015; Ovadnevaite et al., 2014; Ripoll et al., 2015; Minguillon et al., 2015; Poulain et al., 2011b; Poulain et al., 2011a; Huang et al., 2018; Takegawa et al., 2009; Wang et al., 2015; Crenn et al., 2015; Guo et al., 2015; Schlag et al., 2016; Sun et al., 2015). Usually, the comparisons between ACSM and collocated measurements were only performed for a few months up to one year. This might be perfectly adequate to ensure ACSM quality in that period. Only a few systematic comparisons with datasets longer than one year have been reported in the literature (e.g. Fröhlich et al., 2015b; Petit et al., 2015; Parworth et al., 2015; Sun et al., 2015). Ovadnevaite et al. (2014) have written a rare published work that reports long-term AMS comparisons. However, it might not appear sufficiently long to properly evaluate the performance and stability of an instrument designed for long-term monitoring, e.g. covering periods of several years. Therefore, there is really a need for such year-long investigations in order to evaluate the robustness of the instrument independently of calibrations and tuning as well as maintenance activities after technical failures (e.g. such as changing filament, pumps, etc.), seasonal variability, and properly define the limits of such exercises.

A key aspect of such a comparison is the individual upper size cut-off of each instrument. That of an ACSM (as well as the AMS since both are using the same aerodynamic lenses) is considered to be near-PM<sub>1</sub> (vacuum aerodynamic diameter), regarding the approximate 30-40 % transmission efficiency of its aerodynamic lenses at 1 μm (Liu et al., 2007; Takegawa et al., 2009). Recently, a near-PM<sub>2.5</sub> aerodynamic lens has been developed (Xu et al., 2017). However, this new generation of instruments having a near-PM<sub>2.5</sub> cut-off are not within the focus of the present work. Overall, only a limited number of investigations referred to a direct comparison of the ACSM (as well as the AMS) with instruments that have a PM<sub>1</sub> cut-off. From those, multiple external references have been considered in order to compare individual species derived from off-line filter analysis (e.g. Ripoll et al., 2015; Minguillon et al., 2015; Poulain et al., 2011b; Poulain et al., 2011a; Huang et al., 2018), impactors (e.g. Takegawa et al., 2009; Wang et al., 2015), PILS (e.g. Crenn et al., 2015, Guo et al., 2015), and a MARGA (e.g. Schlag et al., 2016). Particle mass closure analysis has also been reported in the literature. It is achieved by adding equivalent Black Carbon mass concentrations (eBC) measured by an Absorption Photometer to the ACSM/AMS ones to obtain PM<sub>1</sub> mass concentrations and compare them with the ones derived from particle number size distributions (PNSD) measured by a MPSS (Mobility Particle Size Spectrometer). One of the main difficulties of a comparison with the MPSS is volume to mass conversion, which requires the density of each detected species (e.g. Ripoll et al 2015, Ortega et al 2016, Bougiatioti et al 2016). To avoid this, some studies have reported a direct comparison of mass concentration vs. volume concentration (e.g. Setyan et al., 2012; DeCarlo et al., 2008; Parworth et al., 2015; Huang et al., 2010). Although this second approach might represent an advantage in providing a direct estimation of the aerosol particle density, the absolute value of the resulting density might become difficult to interpret in some cases because of possible discrepancies between the two instruments types (e.g. Parworth et al., 2015). Although the MPSS is certainly the most popular instrument for particle mass closure analysis, the TEOM-FDMS can be used, since it provides the PM mass concentration directly (Petit et al., 2015; Guerrero et al., 2017).



The aim of the present work is to investigate the long-term stability and comparability between ACSM and collocated and well-established techniques over year-long measurements. Specific attention was put on the influence of the upper size cut-off diameter to better understand how it might affect the validation step and the robustness of the data. Finally, recommendations are provided for better on-site quality assurance and quality control of the ACSM results, which would be useful for either

5 long-term monitoring or intensive campaigns.

## 2. Methodology

### 2.1 Research observatory Melpitz

The atmospheric aerosol measurements were performed at the TROPOS research station Melpitz (51.54 N, 12.93 E, 86 m a.s.l.), 50 km to the northeast of Leipzig, Germany. The station has been in operation since 1992 to examine the effect of atmospheric long-range transport on Central European background air quality (Spindler et al., 2012; Spindler et al., 2013). The site itself is situated on a meadow and is mainly surrounded by agricultural pastures and forests. The Melpitz observatory is part of EMEP (Co-operative Programme for monitoring and evaluation of the long-range transmissions of air pollutants in Europe, Level 3 station, Aas et al., 2012), ACTRIS, ACTRIS-2, GAW (Global Atmosphere Watch of the World Meteorological Organization), and GUAN (German Ultrafine Aerosol Network, Birmili et al., 2015; Birmili et al., 2009; Birmili et al., 2016).

10  
15

All online instruments are set up in the same laboratory container and connected to the same air inlet. This inlet line consists of a PM<sub>10</sub> Anderson impactor located approximately 6 m above ground level and directly followed by an automatic aerosol diffusion dryer to keep the relative humidity on the sampling line below 40 % (Tuch et al., 2009). The aerosol flow is divided among a set of instruments. These instruments include a Multi-Angle Absorption Photometer (MAAP, model 5012, Thermo-Scientific, Petzold and Schönlinner, 2004) to measure the particle light absorption coefficients and the equivalent black carbon (eBC) mass concentration; a dual Mobility Particle Size Spectrometer (TROPOS-type T-MPSS; Birmili et al., 1999; Wiedensohler et al., 2012) to determine the PNSD from 3 to 800 nm (mobility diameter) alternating at ambient temperatures and behind a thermodenuder operating at 300 °C (Wehner et al., 2002); an Aerodynamic Particle Size Spectrometer (APSS; model TSI-3321) to measure the PNSD from 0.8-10 µm (aerodynamic diameter), and a three

20  
25

For a basic overview of the physical and chemical aerosol characterization methods see e.g. Birmili et al. (2008); Spindler et al. (2012); Spindler et al. (2013); Poulain et al. (2014); Poulain et al. (2011b). Physical and optical aerosol instruments are frequently calibrated within the framework of the ECAC. The MPSS is calibrated at the WCCAP (World Calibration Center for Aerosol Physics), following the recommendations given in Wiedensohler et al. (2018). The PNSD uncertainty determined with the MPSS is approximately 10 %. The uncertainty of an APSS is between 10-30 %, depending on the size range (Pfeifer et al., 2016). The uncertainty of the MAAP is also within 10 % as determined by Müller et al. (2011).

30



## 2.2 ACSM

The ACSM (Ng et al., 2011) is connected to the same inlet of the previously described laboratory container. It is based on the same working principle as the widespread Aerodyne Aerosol Mass Spectrometer, AMS (Canagaratna et al., 2007; DeCarlo et al., 2006; Jayne et al., 2000). Compared to the AMS, the ACSM cannot provide size-resolved chemical information. It is equipped with a low-cost residual gas analyzer (RGA) type quadrupole (Pfeiffer Vacuum Prisma plus system) with a unit mass resolution instead of a time-of-flight mass spectrometer. The same aerodynamic lenses as in the AMS are also equipped in the ACSM, with a maximum transmission ranging from 75 to 650 nm, with ca. 30 to 40 % transmission efficiency at 1  $\mu\text{m}$  (Liu et al., 2007). Consequently, the ACSM, like the AMS, provides the chemical composition of non-refractory near- $\text{PM}_{10}$  aerosol particles (organic, nitrate, sulfate, ammonium, and chloride) with a typical time-resolution of 30 min. The ACSM has been permanently operated at the Melpitz since June 2012. The present work will be, however, limited to the period from June 2012 to November 2017. The instrument was sent to the ACMCC (Aerosol Chemical Monitor Calibration Center) near Paris (France) twice to take part of the ECAC intercomparison workshops (Nov-Dec 2013, Crenn et al., 2015; Fröhlich et al., 2015a; and Mar-May 2016, Freney et al., 2019). Overall, the ACSM data covers 80 % of the time the instrument was deployed at Melpitz. Missing days correspond to either instrument failures or maintenance operations. The ACSM measurements and data analysis was made with the latest version of the Data Acquisition (DAQ) and Data Analysis (DAS) software's available at that time (Aerodyne, <https://sites.google.com/site/ariacsm>). The ACSM data was analyzed following the recommendation of manufacturer and applying a chemical time-dependent collection efficiency correction (CDCE) based on the algorithms proposed by Middlebrook et al. (2012) to correct particle loss due to bouncing off the vaporizer before flash vaporization.

20

## 2.3 Off-line chemical characterization

Parallel to the ACSM, the high-volume samplers DIGITEL DHA-80 (Digitel Elektronik AG, Hegnau, Switzerland) collect particles with sizes cutting  $\text{PM}_{2.5}$  and  $\text{PM}_{10}$  on preheated quartz fiber filters (105 °C) (Munktell, Type MK360, Sweden) for 24 hours from midnight to midnight. Samples were performed in a daily-based regime, whereas  $\text{PM}_{10}$  was collected every 6 days. During some specific periods, related to different research projects that took place at the station,  $\text{PM}_{10}$  sampling was also performed on a daily basis, as with  $\text{PM}_{2.5}$  and  $\text{PM}_{10}$ .

After sampling, the filters were conditioned for 48 h at  $20 \pm 2$  °C and  $50 \pm 5$  % RH before being weighted by a microbalance Mettler-Toledo (AT 261). The filters were then extracted with ultrapure water ( $> 18 \text{ M}\Omega\text{cm}$ ) and analyzed through ion chromatography (ICS-3000, Dionex, USA) for water-soluble anions (column AS 18, eluent KOH) and cations (column CS 16, eluent methane sulfonic acid). For further descriptions of sampling and analyzing procedures, see Spindler et al. (2013).

For the chemical quantification of organic carbon (OC) and elemental carbon (EC), the sum of which is total Carbon (TC), a thermo-optical method was used. Rectangular punches (1.5  $\text{cm}^2$ ) of every quartz filter were analyzed for OC and EC using the



Lab OC-EC Aerosol Analyzer (Sunset Laboratory Inc. U.S.A.). The standard temperature protocol EUSAAR2 (Cavalli et al., 2010) was applied to distinguish OC and EC, and the transmittance mode was used for the charring correction. In European networks, like EMEP and ACTRIS, this thermos-optical method is the preferred technique for quartz fiber filters (final temperature 850 °C). Because filter samples were collected over 24 h, an artefact due to the evaporation of the most volatile compounds during warm periods, like ammonium nitrate or some organic, cannot be fully excluded (Schaap et al., 2004; Keck and Wittmaack, 2005).

#### 2.4 Air mass trajectory analysis

A trajectory analysis was made based on 96 h backward trajectories for the altitude of 500 m above model ground with the NOAA Hybrid Single Particle Lagrangian Integrated Trajectory (HYSPLIT-4) model (Draxler and Hess (2004), <http://www.ready.noaa.gov/ready/hysplit4.html>). The trajectories were then analyzed using Zefir 3.7 (Petit et al., 2017) for the identification of potential aerosol sources using the Potential Source Contribution Function (PSCF). Because the filters were collected over 24 h, a total of 12 trajectories were considered for the analysis per day (i.e. every 2 hours), using the enlarge function of Zefir. Finally, the meteorological conditions as available in HYSPLIT during each trajectory were also examined and only the trajectories ending with a Planetary Boundary Layer height (PBL) above 500 m were further considered for analysis. Moreover, trajectories were cut off if they had a precipitation rate of over 1 mm h<sup>-1</sup> and an altitude of above 2000 m.

### 3 Results

To assure the data quality of the ACSM measurements, the results were systematically compared to *i*- daily off-line filter samples (PM<sub>1</sub> and PM<sub>2.5</sub>) of individual species (sulfate, nitrate, ammonium and organic) and *ii*- combined with eBC (MAAP) for mass closure analysis of both off-line filter samplers and on-line MPSS. The accuracy of the comparison and the seasonal variabilities will be discussed in the following. All correlation fits were performed using least the orthogonal fitting approach without forcing it to zero.

#### 3.1 Comparison with off-line chemical composition

A comparison between total PM mass concentrations, sulfate, nitrate, and ammonium over the 5.5 years is plotted in figure 1 for PM<sub>1</sub> and in figure SI-1 for PM<sub>2.5</sub>. The seasonal effect on the fitting's correlation to each species and PM cutting is presented in figures 2 and SI-2 for PM<sub>1</sub> and PM<sub>2.5</sub>, respectively. In the following, chloride will not be considered due to its very low concentrations and limited detection as described by Crenn et al. (2015).

30



### 3.1.1 Sulfate

Over the entire period, the regression slope of the sulfate mass concentration comparison seems to indicate a systematic overestimation of the ACSM compared to PM<sub>1</sub>-filters (slope 1.45, R<sup>2</sup> = 0.59, Fig. 2 and Table SI-1). Better regression slopes were obtained in spring (slope = 0.98, R<sup>2</sup> = 0.74) and summer (slope = 0.87, R<sup>2</sup> = 0.77) than in fall (slope = 1.25, R<sup>2</sup> = 0.58) and winter (slope = 1.57, R<sup>2</sup> = 0.61). However, the overestimation observed throughout the entire period, seems to be strongly influenced by some out-layer days mainly corresponding to three periods taking place in January 2013, October 2015, and February 2017 (these periods are highlighted in Fig. 1). During these periods, the ACSM sulfate mass concentration strongly overestimates the PM<sub>1</sub> one. The correlations with the PM<sub>2.5</sub> sulfate mass concentration (Fig. SI-1 & SI-2) underline the systematic underestimation of the ACSM sulfate concentration throughout the entire period (slope 0.68, R<sup>2</sup> = 0.85), similar to the value reported by Petit et al. (2015) over 2 years of measurements in the region of Paris (France). This overestimation could be associated with the size-cutting difference between the two methods and the presence of not detected sulfate species on the coarse mode, such as sodium sulfate. The seasonal impact on the regression coefficients is less pronounced than in the comparison with PM<sub>1</sub>, with regression slopes ranging from 0.64 (R<sup>2</sup> = 0.85) in spring to 0.94 (R<sup>2</sup> = 0.85) in summer. Contrary to the correlation with PM<sub>1</sub>, no out-layers were identified here.

The following will focus on the ACSM sulfate's overestimation days. There are several reasons that might explain the sulfate overestimation by the ACSM. The first is a technical aspect, since the ACSM has a mass spectrometer with a unit mass resolution, it cannot distinguish between sulfate and organic fragments with the same m/z (for example, C<sub>6</sub>H<sub>8</sub> and/or C<sub>5</sub>H<sub>4</sub>O at m/z 80 for SO<sub>3</sub>, or C<sub>6</sub>H<sub>9</sub> and C<sub>5</sub>H<sub>5</sub>O at m/z 81 for HSO<sub>3</sub>), as already discussed in Budisulistiorini et al. (2014). Therefore, an increase of the organic signal at this m/z might lead to an overestimation of the ACSM sulfate mass concentration. The second possible instrumental artefact is associated with the presence of a higher amount of organo-sulfate during these specific events. Indeed, organo-sulfate compounds lead to similar fragments as inorganic sulfate on AMS mass spectra (e.g. Farmer et al., 2010), which can contribute to the overestimation of the inorganic sulfate mass concentration. However, no particular change of SO<sub>3</sub>/SO and HSO<sub>3</sub>/SO ratios was observed when directly comparing their values before and after events, which can support neither the presence of organo-sulfate nor an increase of organic fragments at m/z 80 and 81. The second aspect is linked to sulfate size distribution. As can be seen in Figure SI-3, the PM<sub>1</sub>:PM<sub>2.5</sub> ratio of the sulfate mass concentration has a pronounced season variability with a mean value of above 0.8 in spring and summer and of 0.6 in winter. The influence of super-μm particles is also supported by the PNSD and PVSD as illustrated in Figure SI-4 for Feb. 2017, which corresponds with the period with the highest discrepancy between the two methods (Fig. 2). In order to investigate a possible dependency on particle mass size distribution, a sensitivity test analysis was performed by investigating the changes of the fitting parameters parallel to the changes of the PM<sub>1</sub>:PM<sub>2.5</sub> ratio on both sulfate and total PM mass concentrations (Fig. 3). In both cases, a clear change in regression slopes as well as intercept values could be observed whenever the PM<sub>1</sub> contribution to PM<sub>2.5</sub> became smaller than 60 %. For days with a PM<sub>1</sub>:PM<sub>2.5</sub> > 60 %, the regression slope ranges from 0.82 and 0.97 with a small intercept value ranging from -0.06 to 0.015 μg m<sup>-3</sup>. As soon as the PM<sub>1</sub> sulfate or the PM mass concentration represents less than 60 %



of the  $PM_{2.5}$ , the ACSM overestimates the  $PM_1$  sulfate. Therefore, the discrepancy between the ACSM and the  $PM_1$  can be attributed to the individual upper size cutting of the two instruments, and it highlights the limits of such a comparison. Consequently, and for the following discussions on sulfate correlation, only the days with a  $PM_1:PM_{2.5}$  ratio of above 60 % will be considered, which still covers more than 80 % of sampling days. The table SI-1 shows the fitting parameters obtained

5 with and without considering the discussed size effect. Interestingly, the  $PM_1:PM_{2.5}$  ratio has a minor influence on nitrate and OC correlation parameters, as will be discussed later on. The resulting correlation parameters show a regression slope of 0.96 (intercept = -0.06 and  $R^2 = 0.77$ , Fig. 2), which supports the results reported by Minguillon et al. (2015) (slope = 1.15) and Ripoll et al. (2015) (slope = 1.12). Seasons do not exercise a significant influence on the correlation between the two instruments, with regression slopes ranging from 0.88 in summer to 1.08 in winter, which supports the results reported by

10 Budisulistiorini et al. (2014) and are better than the ACSM reproducibility uncertainties of 28 % reported by Crenn et al. (2015). The very low intercepts (50 to 4  $ng\ m^{-3}$ ) might indicate a minor contribution of organo-sulfate on the ACSM sulfate (Fig. 2 and Table SI-1). As was already mentioned, the transmission efficiency of the aerodynamic lenses of the ACSM is decreasing from  $\approx 600\ nm$  ( $d_{v0}$ ) to 30-40 % at 1  $\mu m$ . Consequently, the remaining transmission efficiency of the aerodynamic lenses above 1  $\mu m$  influences the sulfate correlation with the  $PM_1$  samples, leading to the reported overestimation of the ACSM

15 sulfate mass concentration on days with a low  $PM_1:PM_{2.5}$  ratio.

To investigate a possible origin of super- $\mu m$  sulfate, trajectory analysis was performed for days that have a difference in sulfate mass concentrations in  $PM_1$  and  $PM_{2.5}$  that is larger than 1  $\mu g\ m^{-3}$  (i.e.  $Sulfate_{PM_{2.5}} - Sulfate_{PM_1} > 1\ \mu g\ m^{-3}$ ) (Fig.4). The air mass density indicates that during these days, the air masses were dominated by two sectors (East and West), with the highest

20 probability in a near Eastern area of Melpitz. This confirms the predominantly low level of the Planetary Boundary Layer height (PBL) as calculated by HYSPLIT, which was below 500 m for approx. 90 % of the time (Figure 4-c), rather indicating local/regional sources than resulting from long-range transport processes. For days that have a connection between calculated trajectories and measurements (e.g.  $PBL > 500\ m$ ), PSCF analysis identified super- $\mu m$  sulfate located inside a narrow corridor starting from Melpitz and going East, then passing over the South of Poland (Fig. 4-b). Since this area is known to host several

25 coal power plants, super- $\mu m$  sulfate might be associated to coal emissions originating from this area.

### 3.1.2 Nitrate

The ACSM nitrate mass concentration tends to overestimate the off-line  $PM_1$  nitrate throughout the entire period (slope = 1.16,  $R^2 = 0.80$ ; Fig. 1 and 2). Such an overestimation of nitrate mass concentrations by the ACSM has already been shown by Ripoll

30 et al. (2015) with a slope of 1.35 ( $R^2 = 0.77$ ) and Minguillon et al. (2015) with a slope 2.8 ( $R^2 = 0.80$ ). A similar conclusion was also drawn by Schlag et al. (2016), during a comparison to MARGA  $PM_1$  measurements. The overall results must be carefully interpreted since a strong seasonal effect has been observed (Fig. 2) with very poor correlation in summer (slope = 6.28,  $R^2 = 0.29$ ) and a strong overestimation during the colder seasons (slope = 1.29,  $R^2 = 0.80$ ). On the one hand, ambient



temperature strongly influences the nitrate mass concentrations on filter samples. Ammonium nitrate is a semi-volatile compound that evaporates, leading to a loss of ammonium nitrate on the filter sample. In an intercomparison study of different sampling supports, Schaap et al. (2004) demonstrated that a quartz filter ( $PM_{2.5}$  and  $PM_{10}$ ) is a suitable material for sampling nitrate as long as the temperature does not exceed 20 °C. This temperature artefact is clearly illustrated in Figure 5, when the variation of the ACSM: $PM_1$  nitrate ratio and the maximum temperature measured during the sampling day are compared. For ambient maximum temperatures above 10 °C, an increase of the ACSM: $PM_1$  ratio can be observed. Here it is imperative to note that the ambient maximum temperature did not reflect the temperature inside the sampler. The highest discrepancy between the two methods corresponds to the warmest days, supporting the temperature artefact. Moreover, this also corresponds to the period with the lowest nitrate mass concentration measured by the ACSM (Fig. 5-b), which might also interfere with the absolute value of the ratio. On the other hand, the nitrate quantification by the ACSM is not free of artefacts. The ACSM's nitrate quantification is mainly based on the signals at  $m/z$  30 (NO) and  $m/z$  46 ( $NO_2$ ), as well as on a minor contribution of  $N^+$  and  $HNO_3^+$  ions in a similar way as for the AMS (Allan et al., 2003). As with sulfate, interferences due to organic contributions at  $m/z$  30 ( $CH_2O^+$  and/or  $C_2H_6^+$ ) and  $m/z$  46 ( $CH_2O_2^+$ ,  $C_2H_6O^+$ ) also cannot be completely excluded. Because the ACSM is working at a unit mass resolution (UMR), it is not possible to distinguish nitrate from organic signals at these two  $m/z$  ratios. The direct consequence is a possible overestimation of the nitrate mass concentration in the UMR during high OA: $NO_3$  periods as shown by Fry et al. (2018). Another source of uncertainties concerning the ACSM nitrate mass concentration is the contribution of organo-nitrates to the nitrate signal, since the nitrate function of the organo-nitrate compounds fragments in a similar way to inorganic nitrate (Farmer et al., 2010). Therefore, the presence of organo-nitrate compounds artificially increases the ACSM-nitrate concentration. Kiendler-Scharr et al. (2016) have already shown that organo-nitrate compounds contribute to a significant fraction of the default AMS- $NO_3$  signal, especially in summer. It represents 57 % and 29 % of the default nitrate measured by an AMS at Melpitz in summer and winter, respectively (Kiendler-Scharr et al., 2016). Since the ACSM and the AMS are based on a similar principle, a simple assumption was made to tentatively correct the ACSM nitrate assuming the following: Firstly, the winter nitrate filter- $PM_1$  mass concentration is free of temperature artefacts, and secondly, the contribution of the organo-nitrate to the ACSM nitrate signal is being constant (29 %) over winter and years as previously reported for winter AMS measurements at the site. The resulting winter nitrate mass concentration has a better correlation to the filter- $PM_1$  (slope 0.88,  $R^2 = 0.77$ , Fig. SI-5). This indirectly confirms the importance of organo-nitrate contributions to the default ACSM nitrate mass concentration during wintertime. Therefore, one should be careful when comparing the ACSM nitrate with an off-line system because of both temperature and organo-nitrate artefacts. Comparing the ACSM with a  $PM_1$  MARGA for a year, Schlag et al. (2016) have obtained a  $R^2$  of 0.96 throughout the year, without discussing seasonal variability. Consequently, all these results tend to indicate that the ACSM inorganic nitrate should properly correlate with the temperature artefact-free  $PM_1$  nitrate measurements, as can be achieved by a PILS or a MARGA for example. Moreover, calculating the difference of nitrate mass concentrations between the ACSM and an online  $PM_1$  system (e.g. PILS or MARGA) might represent a possible way to estimate the organo-nitrate concentration as reported by Xu et al. (2015) using HR-ToF-AMS vs. PILS or by Schlag et al. (2016) using ACSM and MARGA. Due to the



unit mass resolution of the ACSM, direct quantification of particulate organo-nitrate remains a challenging task and more investigations are needed to better understand how organo-nitrate can be detected by the ACSM.

In a first approach, comparisons with the  $PM_{2.5}$  nitrate mass concentration provided better correlation coefficients over the entire period (slope = 0.76,  $R^2 = 0.77$ ), as well as in winter (slope = 0.73,  $R^2 = 0.69$ ), spring (slope = 0.77,  $R^2 = 0.83$ ), and fall (slope = 0.96,  $R^2 = 0.74$ ), compared to  $PM_1$  (Fig. SI-1 and SI-2). Similar to  $PM_1$ , no correlation was found in summer. Here, the temperature effect on the filters as well as on organo-nitrate artefacts seems to have a less pronounced influence. Consequently, the presence of non-volatile nitrate compounds such as sodium nitrate ( $NaNO_3$ ), resulting from the reaction of marine sodium chloride with  $HNO_3$  when marine air masses cross polluted areas (Finlayson-Pitts and Jr, 1986; Pio and Lopes, 1998), might explain the difference of the correlations between  $PM_1$  and  $PM_{2.5}$ . This is supported by the absence of significant effects of the  $PM_1:PM_{2.5}$  nitrate ratio to the fitting parameters when comparing the ACSM nitrate with the  $PM_1$  (Fig. 4). The influence of sodium nitrate at Melpitz has already been discussed in Stieger et al. (2017), comparing  $PM_{10}$  MARGA results with ACSM ones throughout the same period. Consequently, comparisons between the ACSM and  $PM_{2.5}$  nitrate measurements could be strongly biased by coarse mode sodium nitrate that cannot be detected by the ACMS. This might be an important source of artefact, especially for sites under the influence of processed marine air masses, and might lead to a wrong validation of the ACSM nitrate measurements.

### 3.1.3 Ammonium

The ammonium mass concentration measured by the ACSM mostly corresponds to ammonium nitrate and ammonium sulfate salts. Therefore, correlations with off-line systems are something between the two previously discussed ions. During the cold season, the ACSM ammonium mass concentration matches the  $PM_1$  (slope 1.02,  $R^2 = 0.83$ ), which supports the larger fraction of ammonium nitrate in the total PM as well as the size effect of sulfate during wintertime (Fig. 1 and Fig. 2). Although ammonium sulfate dominates during the warmer season, the temperature artefact of ammonium nitrate influences the correlation leading to an under-estimation of the ammonium concentration on the off-line sampler as well as a poor correlation ( $R^2 = 0.49$ ). Similar conclusions can also be drawn when comparing it to the  $PM_{2.5}$  ammonium mass concentration.

### 3.1.4 OM and OC

The ACSM provides organic aerosol (OA) mass concentrations, whereas the organic carbon concentrations (OC) were measured in the filters. The OA mass concentration was compared to the off-line OC mass concentration, which can therefore be considered as a direct estimation of the OM:OC ratio (Fig. 6-a). Correlation between OA and OC is not significantly impacted by the  $PM_1:PM_{2.5}$  threshold ratio of 0.6 as for inorganics (Table SI-1). This supports the fact that organic are mainly distributed on the sub- $\mu m$  size range throughout the year (Fig. SI-3). As expected, a lower OM:OC ratio was obtained in winter



(slope = 1.29,  $R^2 = 0.78$ ), which corresponds with the period with the largest anthropogenic influence. The highest OM:OC ratio was obtained in summer (slope = 2.74,  $R^2 = 0.68$ ), corresponding with the SOA formation maximum. The resulting OM:OC values are larger than usually expected values (e.g. Turpin and Lim, 2001), but such unexpectedly high regression slopes have been observed by Ripoll et al. (2015) (slope of 3.39,  $R^2 = 0.91$ ) and Minguillon et al. (2015) (slope of 4.25,  $R^2 =$   
5 0.82). In a similar way, Budisulistiorini et al. (2014) and references therein have also seen high OM:OC ratio when comparing the ACSM or AMS to the  $PM_{2.5}$  OC from either online or offline measurements. Based on the large dataset available in this study, the time series of the OM:OC ratio (estimated as ACSM-OA divided by  $PM_{1-OC}$ ) as well as its seasonal variation were also investigated (Fig. 6-b and c). The time series also shows some extreme values that are larger than 3, while seasonal means are closer to the expected OM:OC ratios, ranging from 1.66 in winter to 1.98 in summer. Tentative explanations for these  
10 unexpected values might be related to a possible seasonal variability of the relative ionization efficiency (RIE) of organic associated with the change of the aerosol organic composition as demonstrated by Xu et al. (2018).

An estimation of the OM:OC ratio from AMS measurements is normally not done on a direct comparison of organic particle mass concentrations with collocated OC measurements, but rather estimated based on the variability of the  $f_{44}$ , the contribution  
15 of mass  $m/z$  44 (mostly  $CO_2^+$ ) to the total organic signal when not directly calculated through high-resolution mass spectra analysis. Aiken et al. (2007) and Aiken et al. (2008) developed an elemental analysis approach to the AMS mass spectra to provide O:C, H:C and OM:OC ratios based  $f_{44}$ . This method was reinvestigated and improved by Canagaratna et al. (2015) according to the following equations to convert the  $f_{44}$  signal of an AMS into O:C and OM:OC ratios:

$$20 \quad O:C = 0.079 + 4.31 \times f_{44} \quad (1)$$

$$OM:OC = 1.29 \times O:C + 1.17 \quad (2)$$

Equations 1 and 2 were applied in the present dataset to estimate OC mass concentrations from the measured ACSM organic  
25 mass concentration ( $OC_{ACSM}$ ) and to compare them to the  $OC-PM_{1-OC}$  (for the entire dataset: slope = 0.65,  $R^2 = 0.73$ , Fig. 7). As previously shown, a seasonal trend can also be observed here, with a unity regression slope obtained during summer periods (slope = 0.99,  $R^2 = 0.64$ ), whereas a lower slope (0.56,  $R^2 = 0.82$ ) was obtained in winter (Fig. 7 and Table SI-1). Here, the different instrumental and technical uncertainties have to be considered. Contrary to nitrate, temperature seems to have a less significant impact on the ratio between the  $OC_{ACSM}$  and the  $OC_{PM_{1-OC}}$ , as can be seen in figure SI-6. Consequently, the loss of the  
30 most volatile organic species during filter sampling on a warm day should not play a significant role here. As was mentioned above, the seasonal effect might emphasize a possible variability of the organic RIE as well as a possible artefact on the  $CO_2$  signal itself (Pieber et al., 2016; Freney et al., 2019). Moreover, the parameterizations used on Eq. 1 and 2 are only derived from AMS measurements and were not yet tested for the ACSM. Finally, Canagaratna et al. (2015) estimated the uncertainties of Eq. 1 to be around 13 % for SOA aerosol and to be higher for Primary OA. An uncertainty of 19 % in the ACSM-OA mass



concentration can be considered based on the ACSM reproducibility analysis by Crenn et al. (2015). Therefore, the larger discrepancy observed in winter might result from the larger uncertainties of the method due to the increase of anthropogenic emissions on the organic fraction. Despite this agreement between ACSMs, Crenn et al. (2015) showed a large variability concerning the  $f_{44}$  signal itself during the ACSM intercomparison exercise. This variability was attributed to an instrument-  
5 dependent difference of the vaporization conditions. For this reason, the authors did not recommend to systematically use the  $f_{44}$  approach to estimate the O:C ratio, as it can be achieved with the AMS and done here, or to interpret the resulting O:C ratios with caution. Since the  $OC_{ACMS}$  results are well supported by the offline analysis, we can conclude that our ACSM provides a relatively realistic value of the  $f_{44}$  over the considered timeframe and consequently, a reasonable proxy for the OM:OC ratio. However, we cannot rule out that a similar approach would provide the same results when using another ACSM  
10 at Melpitz and/or when applying the present method on another location. Further systematic comparisons between the ACSM and collocated OC- $PM_1$  measurements should be performed in order to better investigate and characterize the suspected instrument vaporization dependency and/or a possible matrix effect depending on the dominant type of aerosol chemical composition at the considered sampling site, which might influence both the  $CO_2$  signal and the organic RIE.

15 Comparison of the  $OC_{ACSM}$  with the OC  $PM_{2.5}$  (Fig. 7) presents a systematic underprediction of the ACSM organic, which can be directly related to the size distribution of organic carbon between  $PM_1$  and  $PM_{2.5}$  (Fig. SI-4). Similar seasonality effects can be observed, which matches the quite constant distribution of the OC between  $PM_1$  and  $PM_{2.5}$  over the course of a year.

### 3.2 Mass closure analysis

20 Before performing a mass closure analysis, the total ACSM particle mass concentration (*i.e.* the sum of organic, nitrate, sulfate, ammonium, and chloride mass concentrations) was completed by adding the eBC  $PM_1$  mass concentration. The eBC ( $PM_{10}$ ) measured by the MAAP was converted to  $PM_1$  by using a factor 0.9, which was obtained by running two MAAPs at Melpitz side by side with different inlets, see Poulain et al. (2011b). The resulting total  $PM_1$  mass, later referred to as the ACSM-MAAP-derived mass concentration, was then compared to the particle mass concentration obtained by weighting filters ( $PM_1$   
25 and  $PM_{2.5}$ ) as well as to the calculated particle mass concentration from the PNSD of the MPSS.

#### 3.2.1 Mass closure with off-line filters

In a similar way to sulfate, the mass closure between the online ACSM-MAAP-derived mass concentration and the offline  $PM_1$  mass concentrations strongly depends on the  $PM_1:PM_{2.5}$  ratio (Fig. 3). Because nitrate and organic did not present such a  
30 dependency to the  $PM_1:PM_{2.5}$  ratio (Fig. 3), the sulfate size distribution should be the main driver of the total mass correlation. Consequently, the same  $PM_1:PM_{2.5}$  threshold of 0.6 is applied in the following for the mass closure analysis and its discussion. It leads to a strong consistency between the online and the offline methods (slope = 1.02,  $R^2 = 0.90$ , Fig. 2 and table SI-1). Our



5 results support those of Petit et al. (2015), who use a PM<sub>1</sub> TEOM-FDMS for mass closure over a 2 years' timeframe (slope 1.06). However, Guerrero et al. (2017) stated that a regression slope of 0.81 could also be found in the PM<sub>1</sub> TEOM-FDMS. However, it is not possible to conclude whether this difference in correlation results between the two studies depend of a location effect or the presence of more coarse mode. Moreover, a possible loss of the more volatile compounds during the heated transmission line of the TEOM-FDMS could also occur.

10 Looking at the different seasons, the regression slopes were always around unit except in fall (slope = 1.31), the overestimation of which will be discussed in the following. Despite a near unity regression slope of 0.96 in summer, the low R<sup>2</sup> and the high intercept value (-3.59 μg m<sup>-3</sup>) both suggest a possible bias between the two methods. Chemical analysis performed on the filter samples can usually not explain their entire mass, leading to the so-call residual mass fraction. This residual mass fraction is made out of all the non-water-soluble compounds such as mineral dust, carbonated or metal ones that are not detected. Here, the residual mass fraction was calculated as the difference between the weighted filter mass and the sum of the detected compounds, applying a constant OM:OC ratio of 1.8 to convert OC into OM (Fig. SI-7). Figure 8 illustrates how this residual mass fraction interferes with the comparison of the ACSM-MAAP-derived mass concentrations. In summer, the residual mass fraction represents a significant part of the PM<sub>1</sub> mass concentration (above 60 %), explaining the low correlation coefficient and the large intercept value in this season. Similar conclusions can be drawn for fall. The increase of residual mass fraction in summer and fall could be associated with a larger resuspension of crustal material on dry and warm days and/or with agricultural activities (e.g. plowing) at these times of the year. Since mineral dust is not detectable by the ACSM, the presence of such compounds in the PM<sub>1</sub> could significantly influence mass closure results and must therefore be considered in such an approach.

20 A comparison with the PM<sub>2.5</sub> mass concentration provides a regression slope of 0.69 (R<sup>2</sup> = 0.77, Fig. SI-2), which matches the comparisons from the literature using PM<sub>2.5</sub> TEOM-FDMS mass concentration (e.g. Sun et al., 2015; Sun et al., 2012). A seasonal effect on the correlation can be observed (Fig. SI-2). In winter, the discrepancy between on-line and off-line techniques becomes more pronounced (slope = 0.65, R<sup>2</sup> = 0.88). This supports the seasonal variation of the PM<sub>1</sub> mass contribution to PM<sub>2.5</sub> (Fig. SI.4) as well as the impact of coarse mode sulfate that was previously mentioned. Similar results were also shown by Sun et al. (2015) when performing mass closure with a PM<sub>2.5</sub> TEOM.

### 3.2.2 Mass closure with PNSD

30 The PNSD is continuously measured parallel to the aerosol mass spectrometer. In order to ensure a comparison between the two systems, the PNSD has to be converted into a volume and mass concentration. Here, the particle mass closure between the ACSM-MAAP and the MPSS (ranging from 10 to 800 nm, mobility diameter) was achieved similarly to what was already done for AMS measurements (e.g. Poulain et al., 2014). First, the conversion of a particle volume concentration into a mass



concentration was achieved by assuming spherical particles and a chemical time-dependent gravimetric particle density based on the following equation from Salcedo et al. (2006):

$$\text{density} = \frac{[\text{Total}_{\text{AMS}} + \text{eBC}]}{\frac{[\text{NO}_3^-] + [\text{SO}_4^{2-}] + [\text{NH}_4^+]}{1.75} + \frac{[\text{Cl}^-]}{1.52} + \frac{[\text{Org}] + [\text{eBC}]}{1.2 + 1.77}} \quad (1)$$

5

Here, the density was assumed to be 1.75 g cm<sup>-3</sup> for ammonium nitrate and ammonium sulfate (Lide, 1991), 1.52 g cm<sup>-3</sup> for ammonium chloride (Lide, 1991), and 1.2 g cm<sup>-3</sup> for organic matter (Turpin and Lim, 2001). Finally, a density of 1.77 g cm<sup>-3</sup> (Park et al., 2004) was applied for eBC. A discussion of eBC density can be found in Poulain et al. (2014).

10 Over 5.5 years of measurements, the ACSM-MAAP-derived mass concentration correlates well with the estimated mass concentrations of the MPSS with a slope of 0.77 ( $R^2 = 0.90$ , Fig. 9). This matches similar previous comparisons at the same place with an AMS (Poulain et al., 2014). However, our results also highlight a non-negligible seasonality effect on mass closure, with a better slope in warmer seasons (summer, slope 0.92,  $R^2 = 0.85$ ) than in cold ones (winter, slope 0.75,  $R^2 = 0.91$ ). A similar seasonality was already reported by Fröhlich et al. (2015b) using a ToF-ACSM at the Jungfrauoch  
15 (Switzerland) during 14-month measurements. The median particle number (Fig. 9-b) and volume (Fig. 9-c) size distributions throughout the winter and summer months emphasize two different behaviors. In winter, the fine mode volume distribution peak occurs around 340 nm, while in summer it's around 250 nm. Moreover, the particle volume size distribution in winter also shows a higher concentration of the largest size bins. This difference corresponds to the higher concentration of super- $\mu\text{m}$  particles in winter as confirmed by the seasonality of the  $\text{PM}_{10}:\text{PM}_{2.5}$  mass ratio (winter 0.73, summer 0.84, Fig. SI-7). The  
20 PNSD provided by the MPSS is corrected from multiple-charged particles artefact in the sub- $\mu\text{m}$  size range, and in case of low contributions of super- $\mu\text{m}$  particles, the multiple-charged particles coming from super- $\mu\text{m}$  particles on the PNSD are negligible. However, in case of a large coarse mode concentration, multiple-charged particles from the super- $\mu\text{m}$  size range might also affect sub- $\mu\text{m}$  size distribution, leading to an overestimation of the PNSD. This interference represents a possible source of artefact for the MPSS in such a case (Birmili et al., 2008). This artefact might be an explanation of the seasonality  
25 trend of the mass closure. An extended particle number size distribution by merging the MPSS and the APSS is presented in Figure SI-4 for February 2017 to illustrate the impact of super- $\mu\text{m}$  particle on size distribution. This period was strongly influenced by coarse mode particles that interfered with the comparison between the ACSM and off-line sulfate and PM as discussed earlier. On the other hand, and as previously mentioned, the transmission efficiency of the aerodynamic lenses of the ACSM decreases to about 30-40 % from  $\approx 650$  nm ( $d_{va}$ ) to 1  $\mu\text{m}$ . Consequently, the ACSM certainly underestimates the  
30 particle mass concentration for the larger size bins compared to the MPSS, which might also have a significant effect on particle mass closure with the MPSS in wintertime.



Assuming spherical particles and a constant density of 1.6, the size cutting of the Digital PM<sub>1</sub> corresponds to a volume equivalent diameter of approx. 790 nm, which is quite similar to the MPSS (800 nm). The comparison between the MPSS-derived mass concentration and the PM<sub>1</sub> filter one also supports our conclusions (Fig. 10). Whereas the correlation slope of 1.79 ( $R^2 = 0.75$ ) over the entire dataset seems to indicate an overestimation of the offline PM<sub>1</sub> compared to the MPSS, the correlation slope is strongly influenced by some winter days. Here, again, the discrepancy between the two methods can be linked directly to the upper size cut of each system. As shown in Figure 10, the discrepancy between the PM<sub>1</sub> and the MPSS-derived mass concentration is always associated with days with a low PM<sub>1</sub>:PM<sub>2.5</sub> ratio corresponding to a larger contribution of the coarse mode particle compared to the other days. This result confirms the individual size cutting effect as well as supports our conclusions on a non-negligible artefact of super- $\mu\text{m}$  multiple charge particles on the estimated MPSS mass concentration on specific winter days. During summertime, the PM<sub>1</sub> filter mass concentrations underestimate those derived from the MPSS, which have to be associated with the already discussed, loss of semi-volatile compounds on the filters.

#### 4 Summary and conclusion

A systematic comparison between the ACSM and collocated measurements (including daily PM<sub>1</sub>, PM<sub>2.5</sub>, and MPSS) over a period of more than 5 years was performed to investigate the robustness of the ACSM as well as to identify the limits of such an exercise and the possible sources of uncertainties and artefacts. The comparison with the offline daily PM<sub>1</sub> samples over the entire period highlights a strong artefact due to the presence of super- $\mu\text{m}$  sulfate. This artefact becomes non-negligible as soon as the PM<sub>1</sub>:PM<sub>2.5</sub> ratio of the sulfate (and subsequently the total PM mass concentration) is below 60 %. The differences were directly associated with the specific size cutting of each instrument and the effect of the remaining transmission efficiency of the aerodynamic lenses of the ACSM above 1  $\mu\text{m}$ . Moreover, similar conclusions were also drawn for the mass closure between the MPSS and PM<sub>1</sub> mass concentrations, confirming individual instrumental upper size cut-off effect. Because this artefact strongly depends on the size distribution of sulfate salts, it certainly depends on the sampling location and the origin of the different aerosol sources. Moreover, this effect should also depend on the aerodynamic lenses itself, which should not all have exactly the same transmission efficiency about 1  $\mu\text{m}$ , leading to a certain instrument dependency. Considering these instrumental limits, the ACSM sulfate mass concentration strongly correlates with the one measured on the filters without any pronounced seasonal effect (slope: 0.96,  $R^2 = 0.77$ ). This also indicates a minor contribution of organo-sulfates to the ACSM sulfate mass concentration at the measurement's site. Consequently, the SO<sub>4</sub>-PM<sub>1</sub> appears to be a crucial parameter to ensure the SO<sub>4</sub>-ACSM validation as well as to support the ACSM's sulfate calibration. In contrast, nitrate mass closure suffers from strong sampling artefacts for both instruments. On the one hand, offline measurements are strongly affected by a temperature effect, leading to the evaporation and loss of ammonium nitrate as was observed for maximum day temperatures of above 10 °C. On the other hand, organo-nitrate compounds lead to a systematic over-prediction of nitrate by the ACSM, which was



clearly demonstrated in winter. Therefore, more investigations on the quantification of organo-nitrate by the ACSM are required in order to reduce this artefact.

The ACSM organic mass concentration correlates with the OC-PM<sub>1</sub> ( $R^2 = 0.66$  to  $0.79$ ), supporting the ACSM organic measurements. The regression slopes have a clear seasonal variability that matches the expected change of the oxidation state of organic throughout the year. Despite the large inter-instrumental variability of the  $f_{44}$  reported by Crenn et al. (2015), the  $f_{44}$  was used to convert the organic mass measured by the ACSM into OC by applying the method proposed by Canagaratna et al. (2015), which was developed for the AMS. The good match between the OC-ACSM and OC-PM<sub>1</sub> (slope ranging from 1.02 in summer to 0.71 in winter with an overall value of 0.74) confirmed that the approach for this instrument and at this sampling place, is also suitable for the ACSM. Nevertheless, more systematic comparisons should be performed in a similar way in different environments to validate our results and to better identify  $f_{44}$  instrumental variability.

Not surprisingly, the comparison to the offline PM<sub>2.5</sub> first highlights the importance of the size cut-off of the filter samples. This is true for all considered species (PM, nitrate, sulfate, ammonium, and organic). Although such conclusions might appear quite trivial, the ACSM as well as the AMS are often compared to PM<sub>2.5</sub> filters. This is certainly the case, because PM<sub>2.5</sub> is the monitoring standard of air quality in several countries like the USA, Canada, and China, contrary to PM<sub>1</sub>. Therefore, for such a comparison, the limitations due to the different size cuttings must be considered.

The total PM<sub>1</sub> mass balance between online (ACSM and MAAP) and offline PM<sub>1</sub> matches throughout the entire time period (slope: 1.02,  $R^2$  0.90) as well as the different seasons when considering the size effect mentioned before. However, non-water-soluble species like dust, metals and carbonate that were not analyzed in the filter samples in this study, and which are also not detected by the ACSM, influence the correlation especially in summer, leading to a lower correlation coefficient during this period ( $R^2 = 0.40$ ). Mass closure with the PNSD certainly represents the best way for in-situ quality control as well as for tracking a possible drift on the ACSM performance. Compared to off-line samples, comparisons with the MPSS do not only have a quite stable correlation over the years and the seasons, but the mass closure between the ACSM and MPSS also presents the main advantage to be done at a near real-time approach, since no further laboratory analyses are needed. Consequently, near real-time mass closure between the ACSM and MPSS should be considered in the near future as a standard way for in-situ quality control of measurements. Moreover, this approach does not remain free of artefacts related to the instrumental upper size cut-off diameter. This should be considered for sampling places with an important coarse mode fraction, in order to considered artefacts induced by both the remaining aerodynamic lens transmission efficiency of the ACSM and the contribution of multiple-charged particles from coarse mode on the PNSD spectra.

Finally, our results clearly emphasize the different limits of a comparison to collocated instruments and the effects of each individual instrumental upper size cut-off diameter. Consequently, there is a need for a better and systematic characterization of the transmission efficiency of the aerodynamic lenses of the ACSM on the upper size range. This knowledge will also certainly be useful to better understand the instrumental variability. Nevertheless, such near real-time comparisons certainly represent the best way to ensure long-term quality assurances of the ACSM measurements, especially at a station where the



ACSM is used for long-term monitoring of particle chemical composition. More systematic comparisons performed in a similar way as in the present work over a long time-period in different environments as well as using different reference methods (e.g. TEOM-FDMS, beta-gauge or a PILS with PM<sub>1</sub> inlet for example) are still needed to better characterize the robustness of the ACSM over a long sampling time.

5

*Data availability:* all data is available upon request to the corresponding author and are deposited on the EBAS-NILU database (<http://ebas.nilu.no/Default.aspx>).

*Authors contributions:* LP, TT, AG, BS collected the data, LP performed data analysis on the ACSM, GS contributed to the evaluation of the off-line dataset and TT to the MPSS. All co-authors participated to the interpretation of the results. LP lead the writing of the manuscript to which authors contributed.

*Competing of interest:* the authors declare that they have no conflict of interest.

#### 15 **Acknowledgments**



This project has received funding from the European Union's Horizon 2020 research and innovation programme within the infrastructure projects ACTRIS (Aerosols, Clouds, and Trace gases Research InfraStructure Network; EU FP7 grant agreement N°262254) and ACTRIS-2 (Aerosols, Clouds, and Trace gases Research InfraStructure, grant agreement N°654109). This work was also supported by the COST Action COLOSSAL CA16109. The physical measurements were also funded by the German Ultrafine Aerosol Network GUAN, which was jointly established with help of the German Federal Environment Ministry (BMU) grants F&E 370343200 (German title: "Erfassung der Zahl feiner und ultrafeiner Partikel in der Außenluft"), 2008–2010, and F&E 371143232 (German title: "Trendanalysen gesundheitsgefährdender Fein- und Ultrafeinstaubfraktionen unter Nutzung der im German Ultrafine Aerosol Network (GUAN) ermittelten Immissionsdaten durch Fortführung und Interpretation der Messreihen") 2012–2014. We also acknowledge the WCCAP (World Calibration Center for Aerosol Physics) as part of the WMO-GAW program. The WCCAP is base-funded by the German Federal Environmental Agency (Umweltbundesamt), Germany. Support by the European Regional Development Funds (EFRE – Europe funds Saxony) is gratefully acknowledged. The authors also thanks R. Rabe especially for technical support in the field and A. Rödger, A. Dietze, and S.Fuchs for numerous laboratory analyses.

#### 30 **References**

Aas, W., Tsyro, S., Bieber, E., Bergström, R., Ceburnis, D., Ellermann, T., Fagerli, H., Frölich, M., Gehrig, R., Makkonen, U., Nemitz, E., Otjes, R., Perez, N., Perrino, C., Prévôt, A. S. H., Putaud, J. P., Simpson, D., Spindler, G., Vana, M., and Yttri,



- K. E.: Lessons learnt from the first EMEP intensive measurement periods, *Atmos. Chem. Phys.*, 12, 8073-8094, doi 10.5194/acp-12-8073-2012, 2012.
- Aiken, A. C., DeCarlo, P. F., and Jimenez, J. L.: Elemental analysis of organic species with electron ionization high-resolution mass spectrometry, *Anal. Chem.*, 79, 8350-8358, doi:10.1021/ac071150w, 2007.
- 5 Aiken, A. C., DeCarlo, P. F., Kroll, J. H., Worsnop, D. R., Huffman, J. A., Docherty, K. S., Ulbrich, I. M., Mohr, C., Kimmel, J. R., Sueper, D., Sun, Y., Zhang, Q., Trimborn, A., Northway, M., Ziemann, P. J., Canagaratna, M. R., Onasch, T. B., Alfarra, M. R., Prevot, A. S. H., Dommen, J., Duplissy, J., Metzger, A., Baltensperger, U., and Jimenez, J. L.: O/C and OM/OC ratios of primary, secondary, and ambient organic aerosols with high-resolution time-of-flight aerosol mass spectrometry, *Environ. Sci. Technol.*, 42, 4478-4485, doi:10.1021/es703009q, 2008.
- 10 Allan, J. D., Alfarra, R. M., Bower, K. N., Williams, P. I., Gallagher, M. W., Jimenez, J. L., McDonald, A. G., Nemitz, E., Canagaratna, M. R., Jayne, J. T., Coe, H., and Worsnop, D. R.: Quantitative sampling using an Aerodyne aerosol mass spectrometer 2. Measurements of fine particulate chemical composition in two U.K. cities, *J. Geophys. Res.*, 108, 4091, doi:10.1029/2002JD002358, 2003.
- Birmili, W., Stratmann, F., and Wiedensohler, A.: Design of a DMA-based size spectrometer for a large particle size range and stable operation, *J. Aerosol Sci.*, 30, 549-553, doi 10.1016/S0021-8502(98)00047-0, 1999.
- Birmili, W., Schepanski, K., Ansmann, A., Spindler, G., Tegen, I., Wehner, B., Nowak, A., Reimer, E., Mattis, I., Müller, K., Brüggemann, E., Gnauk, T., Herrmann, H., Wiedensohler, A., Althausen, D., Schladitz, A., Tuch, T., and Löschau, G.: A case of extreme particulate matter concentrations over Central Europe caused by dust emitted over the southern Ukraine, *Atmos. Chem. Phys.*, 8, 997-1016, doi:10.5194/acp-8-997-2008, 2008.
- 20 Birmili, W., Weinhold, K., Nordmann, S., Wiedensohler, A., Spindler, G., Müller, K., Herrmann, H., Gnauk, T., Pitz, M., Cyrus, J., Flentje, H., Nickel, C., Kuhlbusch, T. A. J., and Löschau, G.: Atmospheric aerosol measurements in the German Ultrafine Aerosol Network (GUAN): Part 1 - soot and particle number size distribution, *Gefahrst. Reinh. Luft.*, 69, 137-145, 2009.
- Birmili, W., Sun, J., Weinhold, K., Merkel, M., Rasch, F., Spindler, G., Wiedensohler, A., Bastian, S., Loschau, G., Schladitz, A., Quass, U., Kuhlbusch, T. A. J., Kaminski, H., Cyrus, J., Pitz, M., Gu, J., Peters, A., Flentje, H., Meinhardt, F., Schwerin, A., Bath, O., Ries, L., Gerwig, H., Wirtz, K., and Weber, S.: Atmospheric aerosol measurements in the German Ultrafine Aerosol Network (GUAN) Part 3: Black Carbon mass and particle number concentrations 2009 to 2014, *Gefahrst. Reinh. Luft.*, 75, 479-488, 2015.
- 25 Birmili, W., Weinhold, K., Rasch, F., Sonntag, A., Sun, J., Merkel, M., Wiedensohler, A., Bastian, S., Schladitz, A., Loschau, G., Cyrus, J., Pitz, M., Gu, J. W., Kusch, T., Flentje, H., Quass, U., Kaminski, H., Kuhlbusch, T. A. J., Meinhardt, F., Schwerin, A., Bath, O., Ries, L., Wirtz, K., and Fiebig, M.: Long-term observations of tropospheric particle number size distributions and equivalent black carbon mass concentrations in the German Ultrafine Aerosol Network (GUAN), *Earth System Science Data*, 8, 355-382, doi:10.5194/essd-8-355-2016, 2016.



- Budisulistiorini, S. H., Canagaratna, M. R., Croteau, P. L., Baumann, K., Edgerton, E. S., Kollman, M. S., Ng, N. L., Verma, V., Shaw, S. L., Knipping, E. M., Worsnop, D. R., Jayne, J. T., Weber, R. J., and Surratt, J. D.: Intercomparison of an Aerosol Chemical Speciation Monitor (ACSM) with ambient fine aerosol measurements in downtown Atlanta, Georgia, *Atmos. Meas. Tech.*, 7, 1929-1941, 10.5194/amt-7-1929-2014, 2014.
- 5 Canagaratna, M. R., Jayne, J. T., Jimenez, J. L., Allan, J. D., Alfarra, M. R., Zhang, Q., Onasch, T. B., Drewnick, F., Coe, H., Middlebrook, A., Delia, A., Williams, L. R., Trimborn, A. M., Northway, M. J., Decarlo, P. F., Kolb, C. E., Davidovits, P., and Worsnop, D. R.: Chemical and microphysical characterization of ambient aerosols with the Aerodyne aerosol mass spectrometer, *Mass Spectrom. Rev.*, 26, 185-222, doi 10.1002/mas.20115, 2007.
- Canagaratna, M. R., Jimenez, J. L., Kroll, J. H., Chen, Q., Kessler, S. H., Massoli, P., Ruiz, L. H., Fortner, E., Williams, L. R.,
- 10 Wilson, K. R., Surratt, J. D., Donahue, N. M., Jayne, J. T., and Worsnop, D. R.: Elemental ratio measurements of organic compounds using aerosol mass spectrometry: characterization, improved calibration, and implications, *Atmos. Chem. Phys.*, 15, 253-272, DOI 10.5194/acp-15-253-2015, 2015.
- Cavalli, F., Viana, M., Yttri, K. E., Genberg, J., and Putaud, J. P.: Toward a standardised thermal-optical protocol for measuring atmospheric organic and elemental carbon: the EUSAAR protocol, *Atmos. Meas. Tech.*, 3, 79-89, DOI 10.5194/amt-3-79-
- 15 2010, 2010.
- Crenn, V., Sciare, J., Croteau, P. L., Verlhac, S., Frohlich, R., Belis, C. A., Aas, W., Auml;ijala, M., Alastuey, A., Artinano, B., Baisnee, D., Bonnaire, N., Bressi, M., Canagaratna, M., Canonaco, F., Carbone, C., Cavalli, F., Coz, E., Cubison, M. J., Esser-Gietl, J. K., Green, D. C., Gros, V., Heikkinen, L., Herrmann, H., Lunder, C., Minguillon, M. C., Mocnik, G., O'Dowd, C. D., Ovadnevaite, J., Petit, J. E., Petralia, E., Poulain, L., Priestman, M., Riffault, V., Ripoll, A., Sarda-Esteve, R., Slowik,
- 20 J. G., Setyan, A., Wiedensohler, A., Baltensperger, U., Prevot, A. S. H., Jayne, J. T., and Favez, O.: ACTRIS ACSM intercomparison - Part 1: Reproducibility of concentration and fragment results from 13 individual Quadrupole Aerosol Chemical Speciation Monitors (Q-ACSM) and consistency with co-located instruments, *Atmos. Meas. Tech.*, 8, 5063-5087, 2015.
- DeCarlo, P. F., Kimmel, J. R., Trimborn, A., Northway, M. J., Jayne, J. T., Aiken, A. C., Gonin, M., Fuhrer, K., Horvath, T.,
- 25 Docherty, K. S., Worsnop, D. R., and Jimenez, J. L.: Field-deployable, high-resolution, time-of-flight aerosol mass spectrometer, *Anal. Chem.*, 78, 8281-8289, doi 10.1021/ac061249n, 2006.
- DeCarlo, P. F., Dunlea, E. J., Kimmel, J. R., Aiken, A. C., Sueper, D., Crounse, J., Wennberg, P. O., Emmons, L., Shinozuka, Y., Clarke, A., Zhou, J., Tomlinson, J., Collins, D. R., Knapp, D., Weinheimer, A. J., Montzka, D. D., Campos, T., and Jimenez, J. L.: Fast airborne aerosol size and chemistry measurements above Mexico City and Central Mexico during the MILAGRO
- 30 campaign, *Atmos. Chem. Phys.*, 8, 4027-4048, 2008.
- Draxler, R., and Hess, G.: Description of the HYSPLIT4 modeling system, NOAA Technical Memorandum, ERL, ARL-224, 2004.



- Farmer, D. K., Matsunaga, A., Docherty, K. S., Surratt, J. D., Seinfeld, J. H., Ziemann, P. J., and Jimenez, J. L.: Response of an aerosol mass spectrometer to organonitrates and organosulfates and implications for atmospheric chemistry, *Proc. Nat. Acad. Sci.*, 107, 6670-6675, doi:10.1073/pnas.0912340107, 2010.
- Finlayson-Pitts, B. J., and Jr, J. N. P.: *Atmospheric chemistry : fundamentals and experimental techniques*, John Wiley & Sons, New York, 1986.
- Freney, E., Zhang, Y., Croteau, P., Amodeo, T., Williams, L., Truong, F., Petit, J.-E., Sciare, J., Sarda-Estève, R., Bonnaire, N., Arumae, T., Aurela, M., Bougiatioti, A., Mihalopoulos, N., Coz, E., Artinano, B., Crenn, V., Elste, T., Heikkinen, L., Poulain, L., Wiedensohler, A., Herrmann, H., Priestman, M., Alastuey, A., Stavroulas, I., Tobler, A., Vasilescu, J., Zanca, N., Canagaratna, M., Carbone, C., Flentje, H., Green, D., Maasikmets, M., Marmureanu, L., Minguillon, M. C., Prevot, A. S. H., Gros, V., Jayne, J., and Favez, O.: The second ACTRIS inter-comparison (2016) for Aerosol Chemical Speciation Monitors (ACSM): Calibration protocols and instrument performance evaluations, *Aerosol Sci. Technol.*, 1-25, 10.1080/02786826.2019.1608901, 2019.
- Fröhlich, R., Crenn, V., Setyan, A., Belis, C. A., Canonaco, F., Favez, O., Riffault, V., Slowik, J. G., Aas, W., Aijala, M., Alastuey, A., Artinano, B., Bonnaire, N., Bozzetti, C., Bressi, M., Carbone, C., Coz, E., Croteau, P. L., Cubison, M. J., Esser-Gietl, J. K., Green, D. C., Gros, V., Heikkinen, L., Herrmann, H., Jayne, J. T., Lunder, C. R., Minguillon, M. C., Mocnik, G., O'Dowd, C. D., Ovadnevaite, J., Petralia, E., Poulain, L., Priestman, M., Ripoll, A., Sarda-Estève, R., Wiedensohler, A., Baltensperger, U., Sciare, J., and Prevot, A. S. H.: ACTRIS ACSM intercomparison - Part 2: Intercomparison of ME-2 organic source apportionment results from 15 individual, co-located aerosol mass spectrometers, *Atmos. Meas. Tech.*, 8, 2555-2576, 2015a.
- Fröhlich, R., Cubison, M. J., Slowik, J. G., Bukowiecki, N., Canonaco, F., Croteau, P. L., Gysel, M., Henne, S., Herrmann, E., Jayne, J. T., Steinbacher, M., Worsnop, D. R., Baltensperger, U., and Prevot, A. S. H.: Fourteen months of on-line measurements of the non-refractory submicron aerosol at the Jungfraujoch (3580 m a.s.l.) - chemical composition, origins and organic aerosol sources, *Atmos. Chem. Phys.*, 15, 11373-11398, 10.5194/acp-15-11373-2015, 2015b.
- Fry, J. L., Brown, S. S., Middlebrook, A. M., Edwards, P. M., Campuzano-Jost, P., Day, D. A., Jimenez, J. L., Allen, H. M., Ryerson, T. B., Pollack, I., Graus, M., Warneke, C., de Gouw, J. A., Brock, C. A., Gilman, J., Lerner, B. M., Dube, W. P., Liao, J., and Welti, A.: Secondary organic aerosol (SOA) yields from NO<sub>3</sub> radical + isoprene based on nighttime aircraft power plant plume transects, *Atmos. Chem. Phys.*, 18, 11663-11682, 10.5194/acp-18-11663-2018, 2018.
- Guerrero, F., Alvarez-Ospina, H., Retama, A., Lopez-Medina, A., Castro, T., and Salcedo, D.: Seasonal changes in the PM1 chemical composition north of Mexico City, *Atmosfera*, 30, 243-258, 10.20937/Atm.2017.30.03.05, 2017.
- Guo, H., Xu, L., Bougiatioti, A., Cerully, K. M., Capps, S. L., Hite, J. R., Carlton, A. G., Lee, S. H., Bergin, M. H., Ng, N. L., Nenes, A., and Weber, R. J.: Fine-particle water and pH in the southeastern United States, *Atmos. Chem. Phys.*, 15, 5211-5228, 10.5194/acp-15-5211-2015, 2015.
- Gurjar, B. R., Jain, A., Sharma, A., Agarwal, A., Gupta, A., Nagpure, A. S., and Lelieveld, J.: Human health risks in megacities due to air pollution, *Atmos. Environ.*, 44, 4606-4613, doi:10.1016/j.atmosenv.2010.08.011, 2010.



- Huang, S., Wu, Z., Poulain, L., van Pinxteren, M., Merkel, M., Assmann, D., Herrmann, H., and Wiedensohler, A.: Source apportionment of the organic aerosol over the Atlantic Ocean from 53° N to 53° S: significant contributions from marine emissions and long-range transport, *Atmos. Chem. Phys.*, 18043-18062, doi.org/10.5194/acp-18-18043, 2018.
- Huang, X. F., He, L. Y., Hu, M., Canagaratna, M. R., Sun, Y., Zhang, Q., Zhu, T., Xue, L., Zeng, L. W., Liu, X. G., Zhang, Y. H., Jayne, J. T., Ng, N. L., and Worsnop, D. R.: Highly time-resolved chemical characterization of atmospheric submicron particles during 2008 Beijing Olympic Games using an Aerodyne High-Resolution Aerosol Mass Spectrometer, *Atmos. Chem. Phys.*, 10, 8933-8945, 10.5194/acp-10-8933-2010, 2010.
- Jayne, J. T., Leard, D. C., Zhang, X., Davidovits, P., Smith, K. A., Kolb, C. E., and Worsnop, D. R.: Development of an Aerosol Mass Spectrometer for size and composition analysis of submicron particles, *Aerosol Sci. Technol.*, 33, 49-70, 2000.
- Keck, L., and Wittmaack, K.: Effect of filter type and temperature on volatilisation losses from ammonium salts in aerosol matter, *Atmos. Environ.*, 39, 4093-4100, 10.1016/j.atmosenv.2005.03.029, 2005.
- Kiendler-Scharr, A., Mensah, A. A., Friese, E., Topping, D., Nemitz, E., Prevot, A. S. H., Aijala, M., Allan, J., Canonaco, F., Canagaratna, M., Carbone, S., Crippa, M., Dall'Osto, M., Day, D. A., De Carlo, P., Di Marco, C. F., Elbern, H., Eriksson, A., Freney, E., Hao, L., Herrmann, H., Hildebrandt, L., Hillamo, R., Jimenez, J. L., Laaksonen, A., McFiggans, G., Mohr, C., O'Dowd, C., Otjes, R., Ovadnevaite, J., Pandis, S. N., Poulain, L., Schlag, P., Sellegri, K., Swietlicki, E., Tiitta, P., Vermeulen, A., Wahner, A., Worsnop, D., and Wu, H. C.: Ubiquity of organic nitrates from nighttime chemistry in the European submicron aerosol, *Geophys. Res. Lett.*, 43, 7735-7744, 2016.
- Lelieveld, J., Evans, J. S., Fnais, M., Giannadaki, D., and Pozzer, A.: The contribution of outdoor air pollution sources to premature mortality on a global scale, *Nature*, 525, 367+, 2015.
- Lide, D. R.: *CRC Handbook of Chemistry and Physics*, CRC Press Inc., USA, 1991.
- Liu, P. S. K., Deng, R., Smith, K. A., Williams, L. R., Jayne, J. T., Canagaratna, M. R., Moore, K., Onasch, T. B., Worsnop, D. R., and Deshler, T.: Transmission efficiency of an aerodynamic focussing lens system: Comparison of model calculations and laboratory measurements for the aerodyne aerosol mass spectrometer, *Aerosol Sci. Technol.*, 41, doi:10.1080/02786820701422278, 2007.
- Middlebrook, A. M., Bahreini, R., Jimenez, J. L., and Canagaratna, M. R.: Evaluation of Composition-Dependent Collection Efficiencies for the Aerodyne Aerosol Mass Spectrometer using Field Data, *Aerosol Sci. Technol.*, 46, 258-271, doi:10.1080/02786826.2011.620041, 2012.
- Minguillon, M. C., Ripoll, A., Perez, N., Prevot, A. S. H., Canonaco, F., Querol, X., and Alastuey, A.: Chemical characterization of submicron regional background aerosols in the western Mediterranean using an Aerosol Chemical Speciation Monitor, *Atmos. Chem. Phys.*, 15, 6379-6391, 10.5194/acp-15-6379-2015, 2015.
- Müller, T., Henzing, J. S., de Leeuw, G., Wiedensohler, A., Alastuey, A., Angelov, H., Bizjak, M., Coen, M. C., Engstrom, J. E., Gruening, C., Hillamo, R., Hoffer, A., Imre, K., Ivanow, P., Jennings, G., Sun, J. Y., Kalivitis, N., Karlsson, H., Komppula, M., Laj, P., Li, S. M., Lunder, C., Marinoni, A., dos Santos, S. M., Moerman, M., Nowak, A., Ogren, J. A., Petzold, A., Pichon, J. M., Rodriguez, S., Sharma, S., Sheridan, P. J., Teinila, K., Tuch, T., Viana, M., Virkkula, A., Weingartner, E., Wilhelm, R.,



- and Wang, Y. Q.: Characterization and intercomparison of aerosol absorption photometers: result of two intercomparison workshops, *Atmos. Meas. Tech.*, 4, 245-268, 10.5194/amt-4-245-2011, 2011.
- Ng, N. L., Herndon, S. C., Trimborn, A., Canagaratna, M. R., Croteau, P. L., Onasch, T. B., Sueper, D., Worsnop, D. R., Zhang, Q., Sun, Y. L., and Jayne, J. T.: An Aerosol Chemical Speciation Monitor (ACSM) for Routine Monitoring of the  
5 Composition and Mass Concentrations of Ambient Aerosol, *Aerosol Sci. Technol.*, 45, 780-794, doi 10.1080/02786826.2011.560211, 2011.
- Ostro, B., Feng, W. Y., Broadwin, R., Green, S., and Lipsett, M.: The effects of components of fine particulate air pollution on mortality in California: Results from CALFINE, *Environ. Health Perspect.*, 115, 13-19, doi:10.1289/Ehp.9281, 2007.
- Ovadnevaite, J., Ceburnis, D., Leinert, S., Dall'Osto, M., Canagaratna, M., O'Doherty, S., Berresheim, H., and O'Dowd, C.:  
10 Submicron NE Atlantic marine aerosol chemical composition and abundance: Seasonal trends and air mass categorization, *Journal of Geophysical Research-Atmospheres*, 119, 11850-11863, 10.1002/2013jd021330, 2014.
- Park, K., Kittelson, D. B., Zachariah, M. R., and McMurry, P. H.: Measurement of inherent material density of nanoparticle agglomerates, *J. Nanopart. Res.*, 6, 267-272, doi:10.1023/B:NANO.0000034657.71309.e6, 2004.
- Parworth, C., Fast, J., Mei, F., Shippert, T., Sivaraman, C., Tilp, A., Watson, T., and Zhang, Q.: Long-term measurements of  
15 submicrometer aerosol chemistry at the Southern Great Plains (SGP) using an Aerosol Chemical Speciation Monitor (ACSM), *Atmos. Environ.*, 106, 43-55, 10.1016/j.atmosenv.2015.01.060, 2015.
- Petit, J. E., Favez, O., Sciare, J., Crenn, V., Sarda-Estève, R., Bonnaire, N., Mocnik, G., Dupont, J. C., Haeffelin, M., and Leoz-Garziandia, E.: Two years of near real-time chemical composition of submicron aerosols in the region of Paris using an Aerosol Chemical Speciation Monitor (ACSM) and a multi-wavelength Aethalometer, *Atmos. Chem. Phys.*, 15, 2985-3005,  
20 10.5194/acp-15-2985-2015, 2015.
- Petit, J. E., Favez, O., Albinet, A., and Canonaco, F.: A user-friendly tool for comprehensive evaluation of the geographical origins of atmospheric pollution: Wind and trajectory analyses, *Environ. Modell. Softw.*, 88, 183-187, 10.1016/j.envsoft.2016.11.022, 2017.
- Petzold, A., and Schönlinner, M.: Multi-angle absorption photometry - a new method for the measurement of aerosol light  
25 absorption and atmospheric black carbon, *J. Aerosol Sci.*, 35, 421-441, doi: 10.1016/j.jaerosci.2003.09.005, 2004.
- Pfeifer, S., Müller, T., Weinhold, K., Zikova, N., dos Santos, S. M., Marinoni, A., Bischof, O. F., Kykal, C., Ries, L., Meinhardt, F., Aalto, P., Mihalopoulos, N., and Wiedensohler, A.: Intercomparison of 15 aerodynamic particle size spectrometers (APS 3321): uncertainties in particle sizing and number size distribution, *Atmos. Meas. Tech.*, 9, 1545-1551, 10.5194/amt-9-1545-2016, 2016.
- 30 Pieber, S. M., El Haddad, I., Slowik, J. G., Canagaratna, M. R., Jayne, J. T., Platt, S. M., Bozzetti, C., Daellenbach, K. R., Frohlich, R., Vlachou, A., Klein, F., Dommen, J., Miljevic, B., Jimenez, J. L., Worsnop, D. R., Baltensperger, U., and Prevot, A. S. H.: Inorganic Salt Interference on CO<sub>2</sub><sup>+</sup> in Aerodyne AMS and ACSM Organic Aerosol Composition Studies, *Environ. Sci. Technol.*, 50, 10494-10503, 10.1021/acs.est.6b01035, 2016.



- Pio, C. A., and Lopes, D. A.: Chlorine loss from marine aerosol in a coastal atmosphere, *Journal of Geophysical Research-Atmospheres*, 103, 25263-25272, Doi 10.1029/98jd02088, 1998.
- Poulain, L., Iinuma, Y., Müller, K., Birmili, W., Weinhold, K., Brüggemann, E., Gnauk, T., Hausmann, A., Löschau, G., Wiedensohler, A., and Herrmann, H.: Diurnal variations of ambient particulate wood burning emissions and their contribution to the concentration of Polycyclic Aromatic Hydrocarbons (PAHs) in Seiffen, Germany, *Atmos. Chem. Phys.*, 11, 12697-12713, doi: 10.5194/acp-11-12697-2011, 2011a.
- Poulain, L., Spindler, G., Birmili, W., Plass-Dülmer, C., Wiedensohler, A., and Herrmann, H.: Seasonal and diurnal variations of particulate nitrate and organic matter at the IfT research station Melpitz, *Atmos. Chem. Phys.*, 11, 12579-12599, doi:10.5194/acp-11-12579-2011, 2011b.
- 10 Poulain, L., Birmili, W., Canonaco, F., Crippa, M., Wu, Z. J., Nordmann, S., Spindler, G., Prevot, A. S. H., Wiedensohler, A., and Herrmann, H.: Chemical mass balance of 300 degrees C non-volatile particles at the tropospheric research site Melpitz, Germany, *Atmos. Chem. Phys.*, 14, 10145-10162, doi:10.5194/acp-14-10145-2014, 2014.
- Ripoll, A., Minguillon, M. C., Pey, J., Jimenez, J. L., Day, D. A., Sosedova, Y., Canonaco, F., Prevot, A. S. H., Querol, X., and Alastuey, A.: Long-term real-time chemical characterization of submicron aerosols at Montsec (southern Pyrenees, 1570 m a.s.l.), *Atmos. Chem. Phys.*, 15, 2935-2951, 10.5194/acp-15-2935-2015, 2015.
- 15 Salcedo, D., Onasch, T. B., Dzepina, K., Canagaratna, M. R., Zhang, Q., Huffman, J. A., DeCarlo, P. F., Jayne, J. T., Mortimer, P., Worsnop, D. R., Kolb, C. E., Johnson, K. S., Zuberi, B., Marr, L. C., Volkamer, R., Molina, L. T., Molina, M. J., Cardenas, B., Bernabe, R. M., Marquez, C., Gaffney, J. S., Marley, N. A., Laskin, A., Shutthanandan, V., Xie, Y., Brune, W., Leshner, R., Shirley, T., and Jimenez, J. L.: Characterization of ambient aerosols in Mexico City during the MCMA-2003 campaign with  
20 Aerosol Mass Spectrometry: results from the CENICA Supersite, *Atmos. Chem. Phys.*, 6, 925 - 946, doi:10.5194/acp-6-925-2006, 2006.
- Schaap, M., Spindler, G., Schulz, M., Acker, K., Maenhaut, W., Berner, A., Wieprecht, W., Streit, N., Müller, K., Brüggemann, E., Chi, X., Putaud, J. P., Hittenberger, R., Puxbaum, H., Baltensperger, U., and ten Brink, H.: Artefacts in the sampling of nitrate studied in the "INTERCOMP" campaigns of EUROTRAC-AEROSOL, *Atmos. Environ.*, 38, 6487-6496,  
25 10.1016/j.atmosenv.2004.08.026, 2004.
- Schlag, P., Kiendler-Scharr, A., Blom, M. J., Canonaco, F., Henzing, J. S., Moerman, M., Prevot, A. S. H., and Holzinger, R.: Aerosol source apportionment from 1-year measurements at the CESAR tower in Cabauw, the Netherlands, *Atmos. Chem. Phys.*, 16, 8831-8847, 10.5194/acp-16-8831-2016, 2016.
- Setyan, A., Zhang, Q., Merkel, M., Knighton, W. B., Sun, Y., Song, C., Shilling, J. E., Onasch, T. B., Herndon, S. C., Worsnop, D. R., Fast, J. D., Zaveri, R. A., Berg, L. K., Wiedensohler, A., Flowers, B. A., Dubey, M. K., and Subramanian, R.: Characterization of submicron particles influenced by mixed biogenic and anthropogenic emissions using high-resolution aerosol mass spectrometry: results from CARES, *Atmos. Chem. Phys.*, 12, 8131-8156, doi:10.5194/acp-12-8131-2012, 2012.

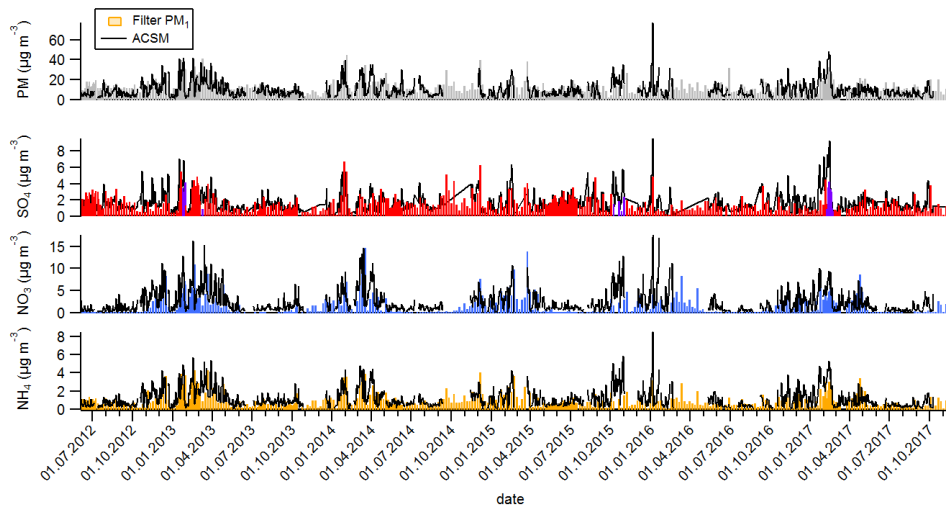


- Spindler, G., Gnauk, T., Grüner, A., Iinuma, Y., Müller, K., Scheinhardt, S., and Herrmann, H.: Size-segregated characterization of PM<sub>10</sub> at the EMEP site Melpitz (Germany) using a five-stage impactor: a six year study, *J. Atmos. Chem.*, 69, 127-157, doi:10.1007/s10874-012-9233-6, 2012.
- Spindler, G., Grüner, A., Müller, K., Schlimper, S., and Herrmann, H.: Long-term size-segregated particle (PM<sub>10</sub>, PM<sub>2.5</sub>, PM<sub>1</sub>) characterization study at Melpitz - influence of air mass inflow, weather conditions and season, *J. Atmos. Chem.*, 70, 165-195, doi:10.1007/s10874-013-9263-8, 2013.
- Stieger, B., Spindler, G., Fahlbusch, B., Müller, K., Grüner, A., Poulain, L., Thöni, L., Seitler, E., Wallasch, M., and Herrmann, H.: Measurements of PM<sub>10</sub> ions and trace gases with the online system MARGA at the research station Melpitz in Germany – A five-year study, *J. Atmos. Chem.*, 10.1007/s10874-017-9361-0, 2017.
- 10 Sun, Y. L., Zhang, Q., Schwab, J. J., Yang, T., Ng, N. L., and Demerjian, K. L.: Factor analysis of combined organic and inorganic aerosol mass spectra from high resolution aerosol mass spectrometer measurements, *Atmos. Chem. Phys.*, 12, 8537-8551, 10.5194/acp-12-8537-2012, 2012.
- Sun, Y. L., Wang, Z. F., Du, W., Zhang, Q., Wang, Q. Q., Fu, P. Q., Pan, X. L., Li, J., Jayne, J., and Worsnop, D. R.: Long-term real-time measurements of aerosol particle composition in Beijing, China: seasonal variations, meteorological effects, and source analysis, *Atmos. Chem. Phys.*, 15, 10149-10165, 10.5194/acp-15-10149-2015, 2015.
- 15 Takegawa, N., Miyakawa, T., Watanabe, M., Kondo, Y., Miyazaki, Y., Han, S., Zhao, Y., van Pinxteren, D., Brüggemann, E., Gnauk, T., Herrmann, H., Xiao, R., Deng, Z., Hu, M., Zhu, T., and Zhang, Y.: Performance of an Aerodyne Aerosol Mass Spectrometer (AMS) during Intensive Campaigns in China in the Summer of 2006, *Aerosol Sci. Technol.*, 43, 189-204, doi:10.1080/02786820802582251, 2009.
- 20 Tuch, T. M., Haudek, A., Müller, T., Nowak, A., Wex, H., and Wiedensohler, A.: Design and performance of an automatic regenerating adsorption aerosol dryer for continuous operation at monitoring sites, *Atmos. Meas. Tech.*, 2, 417-422, doi:10.5194/amt-2-417-2009, 2009.
- Turpin, B. J., and Lim, H.-J.: Species contributions to PM<sub>2.5</sub> mass concentrations: revisiting common assumptions for estimating organic mass, *Aerosol Sci. Technol.*, 35, 302-610, doi:10.1080/02786820119445, 2001.
- 25 Wang, Q. Q., Sun, Y. L., Jiang, Q., Du, W., Sun, C. Z., Fu, P. Q., and Wang, Z. F.: Chemical composition of aerosol particles and light extinction apportionment before and during the heating season in Beijing, China, *Journal of Geophysical Research-Atmospheres*, 120, 12708-12722, 10.1002/2015jd023871, 2015.
- Wehner, B., Philippin, S., and Wiedensohler, A.: Design and calibration of a thermodenuder with an improved heating unit to measure the size-dependent volatile fraction of aerosol particles, *J. Aerosol Sci.*, 33, 1087-1093, 2002.
- 30 Wiedensohler, A., Birmili, W., Nowak, A., Sonntag, A., Weinhold, K., Merkel, M., Wehner, B., Tuch, T., Pfeifer, S., Fiebig, M., Fjaraa, A. M., Asmi, E., Sellegri, K., Depuy, R., Venzac, H., Villani, P., Laj, P., Aalto, P., Ogren, J. A., Swietlicki, E., Williams, P., Roldin, P., Quincey, P., Hüglin, C., Fierz-Schmidhauser, R., Gysel, M., Weingartner, E., Riccobono, F., Santos, S., Gruning, C., Faloon, K., Beddows, D., Harrison, R. M., Monahan, C., Jennings, S. G., O'Dowd, C. D., Marinoni, A., Horn, H. G., Keck, L., Jiang, J., Scheckman, J., McMurry, P. H., Deng, Z., Zhao, C. S., Moerman, M., Henzing, B., de Leeuw, G.,



- Loschau, G., and Bastian, S.: Mobility particle size spectrometers: harmonization of technical standards and data structure to facilitate high quality long-term observations of atmospheric particle number size distributions, *Atmos. Meas. Tech.*, 5, 657-685, doi 10.5194/amt-5-657-2012, 2012.
- Wiedensohler, A., Wiesner, A., Weinhold, K., Birmili, W., Hermann, M., Merkel, M., Muller, T., Pfeifer, S., Schmidt, A.,  
5 Tuch, T., Velarde, F., Quincey, P., Seeger, S., and Nowak, A.: Mobility particle size spectrometers: Calibration procedures and measurement uncertainties, *Aerosol Sci. Technol.*, 52, 146-164, 10.1080/02786826.2017.1387229, 2018.
- Xu, L., Guo, H. Y., Boyd, C. M., Klein, M., Bougiatioti, A., Cerully, K. M., Hite, J. R., Isaacman-VanWertz, G., Kreisberg, N. M., Knote, C., Olson, K., Koss, A., Goldstein, A. H., Hering, S. V., de Gouw, J., Baumann, K., Lee, S. H., Nenes, A., Weber, R. J., and Ng, N. L.: Effects of anthropogenic emissions on aerosol formation from isoprene and monoterpenes in the  
10 southeastern United States, *Proceedings of the National Academy of Sciences of the United States of America*, 112, 37-42, 10.1073/pnas.1417609112, 2015.
- Xu, W., Croteau, P., Williams, L., Canagaratna, M., Onasch, T., Cross, E., Zhang, X., Robinson, W., Worsnop, D., and Jayne, J.: Laboratory characterization of an aerosol chemical speciation monitor with PM<sub>2.5</sub> measurement capability, *Aerosol Sci. Technol.*, 51, 69-83, 10.1080/02786826.2016.1241859, 2017.
- 15 Xu, W., Lambe, A., Silva, P., Hu, W. W., Onasch, T., Williams, L., Croteau, P., Zhang, X., Renbaum-Wolff, L., Fortner, E., Jimenez, J. L., Jayne, J., Worsnop, D., and Canagaratna, M.: Laboratory evaluation of species-dependent relative ionization efficiencies in the Aerodyne Aerosol Mass Spectrometer, *Aerosol Sci. Technol.*, 52, 626-641, 10.1080/02786826.2018.1439570, 2018.

20



5 **Figure 1:** Time series ACSM (daily averaged, black line) and 24 h PM<sub>1</sub> filter samples (colored bars) for the total particle mass concentration, the mass concentration of sulfate, nitrate and ammonium. The particulate matter (PM) corresponds with the sum of ACSM species and eBC<sub>PM1</sub> for the on-line instrument and the PM<sub>1</sub> filter mass for the off-line samples.

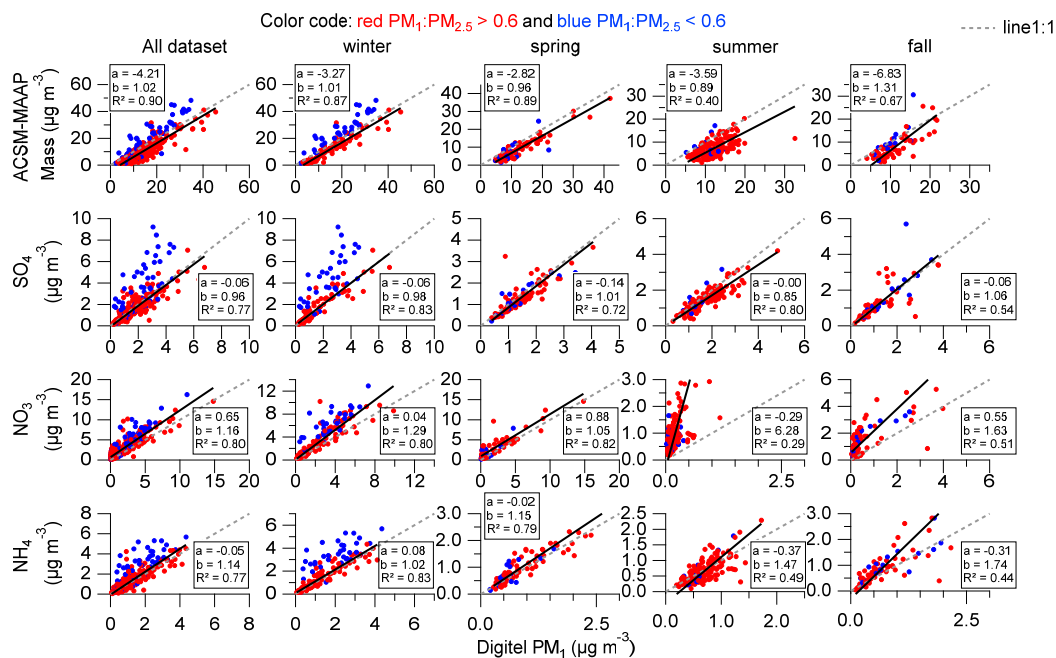


**Figure 2:** Seasonal variability of the comparison between on-line and off-line  $PM_1$  aerosol measurements. The color coding indicates whether the ratio  $PM_1:PM_{2.5}$  total mass concentration is above (red) or below (blue) the selected threshold value of 0.6 (see discussion in section 3.1.1.). Dotted grey lines show the line 1:1 and full black lines and parameters the least orthogonal distance fit ( $y = a + bx$ ).

5 Please note the different axis ranges for the same species.

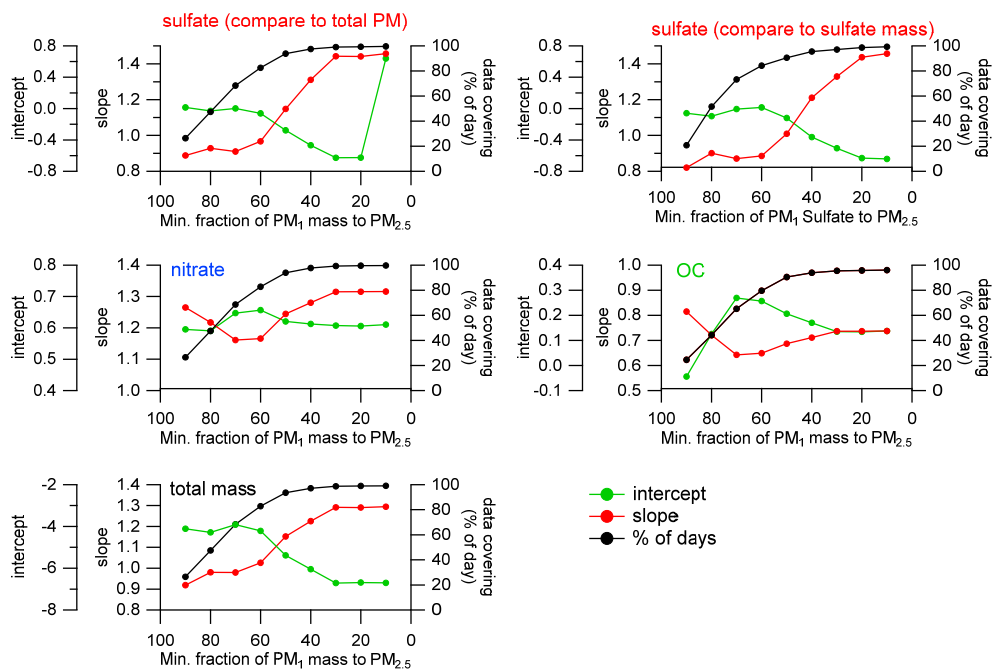
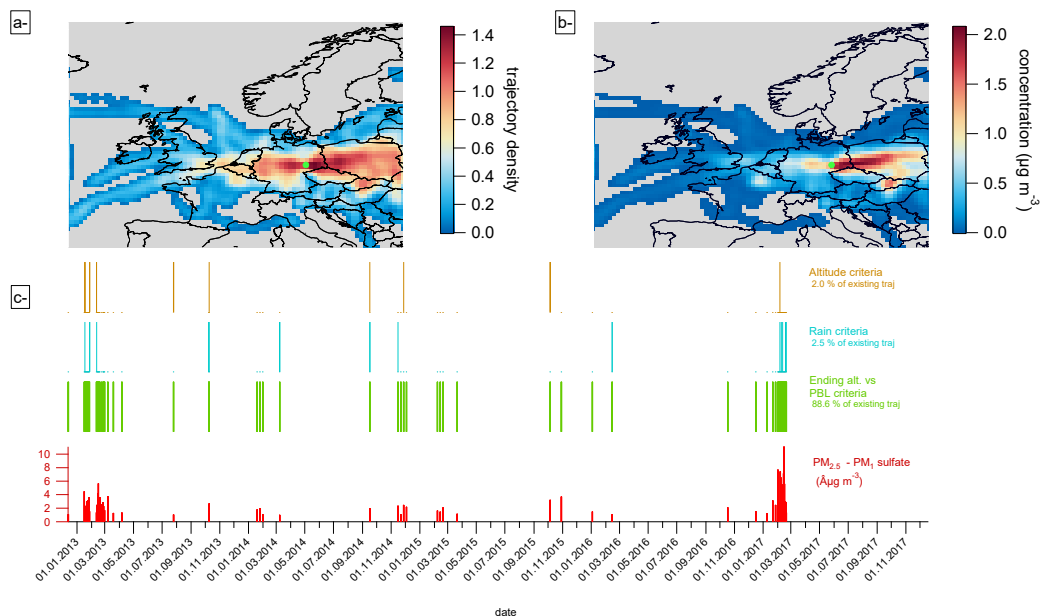
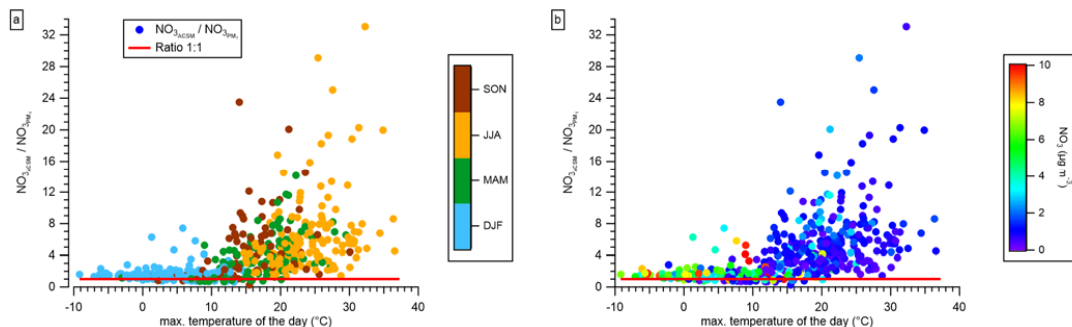


**Figure 3:** Sensitivity analysis of the correlation between ACSM and PM<sub>1</sub> sulfate, nitrate, OC, and total mass concentration depending on the PM<sub>1</sub>:PM<sub>2.5</sub> ratio of the total mass concentration in the range 90 – 10 %. The influence of sulfate distribution on PM<sub>1</sub> and PM<sub>2.5</sub> was also investigated (top left).

5



5 **Figure 4:** Trajectory analysis for days that have a different  $\text{PM}_{2.5} - \text{PM}_1$  sulfate mass concentration above  $1 \mu\text{g m}^{-3}$ . a- Trajectory density, b- potential source maps (PSCF). The panel c- shows the time series of the considered sulfate mass concentration (bottom) and the colored bars show the days when the trajectories did not pass the different trajectory cut-off options: Altitude above 2000 m (top brown), rain  $> 1 \text{ mm h}^{-1}$  (middle blue) and PBL above the station  $< 500 \text{ m}$  (bottom green).



10 **Figure 5:** ACSM:PM<sub>1</sub> ratio nitrate mass concentration compared to the maximum temperature of the corresponding sampling day. The color code corresponds to the different seasons (a) and the total nitrate mass concentration of the ACSM (b).

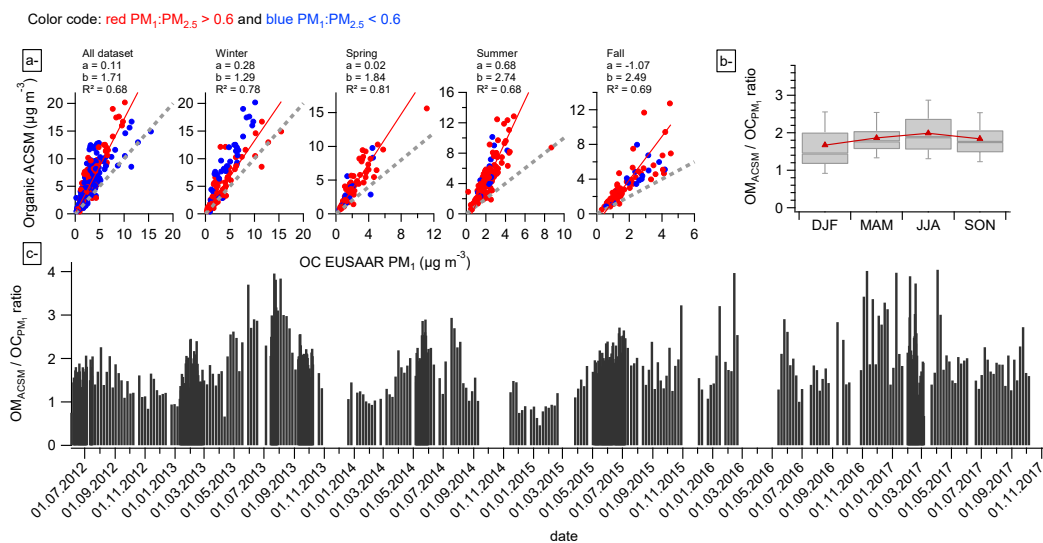


**Figure 6: Correlation between ACSM organic mass concentrations and off-line OC  $PM_1$  (a), seasonal variability of the estimated  $OM_{ACSM}:OC_{PM_1}$  ratio (b), and corresponding (c) shows its time series.**

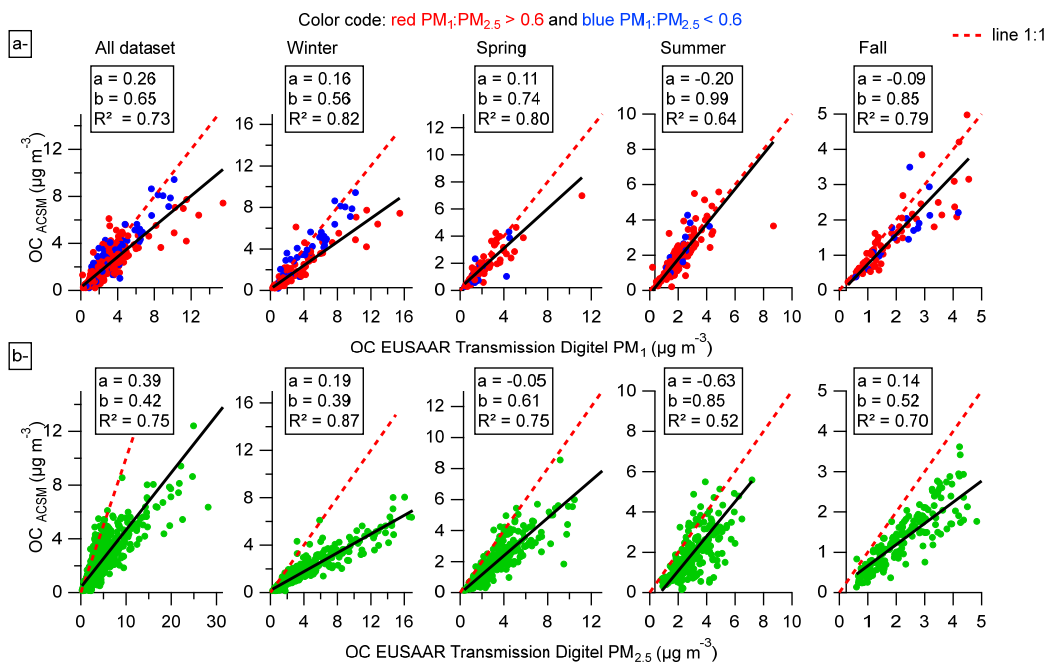


Figure 7: Correlations between the estimated  $OC_{ACSM}$  mass concentrations and the off-line  $PM_1$  (a) and  $PM_{2.5}$  (b) EUSAAR transmission OC mass concentration for the entire period and the different seasons. Black lines show the least orthogonal linear fit and the red dotted lines the line 1:1.

5

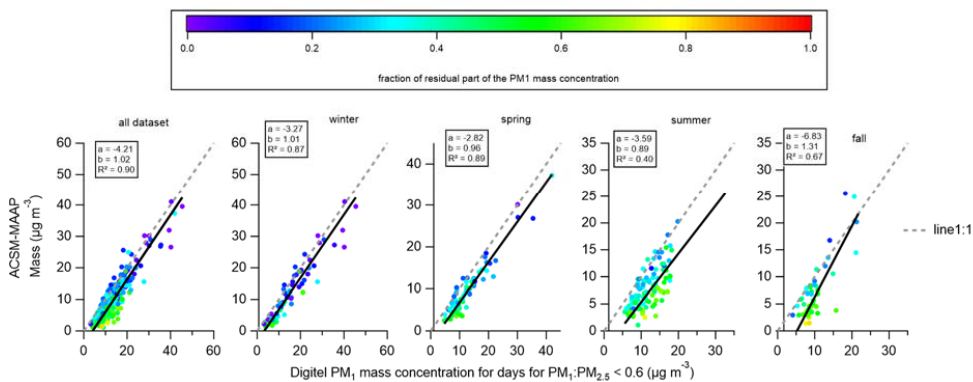


Figure 8: Influence of the residual mass fraction on the  $PM_1$  filter to the mass closure with online ACSM-MAAP-derived mass concentration.

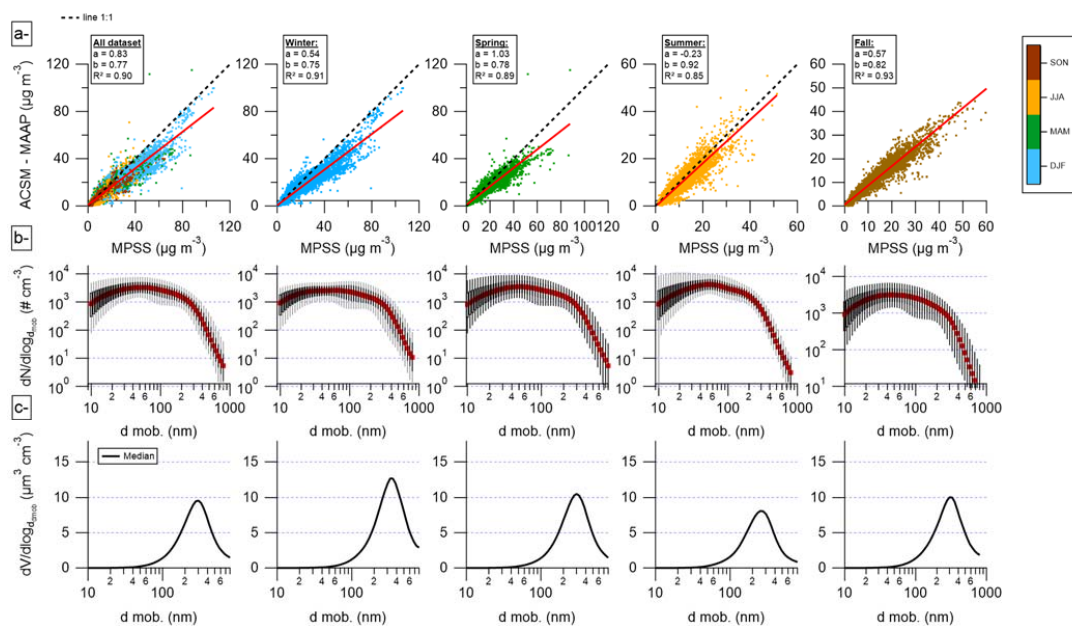


Figure 9: Comparison between measured ACSM-MAAP-derived mass concentrations and the MPSS-derived mass concentrations for the entire period and the different seasons. In panel a-, the correlation curves (red lines) were calculated using the least orthogonal distance fit method. b- Median number size distribution (red) with 10-90 (grey lines) and 25-75 (black boxes) percentiles. c- Median volume size distribution.

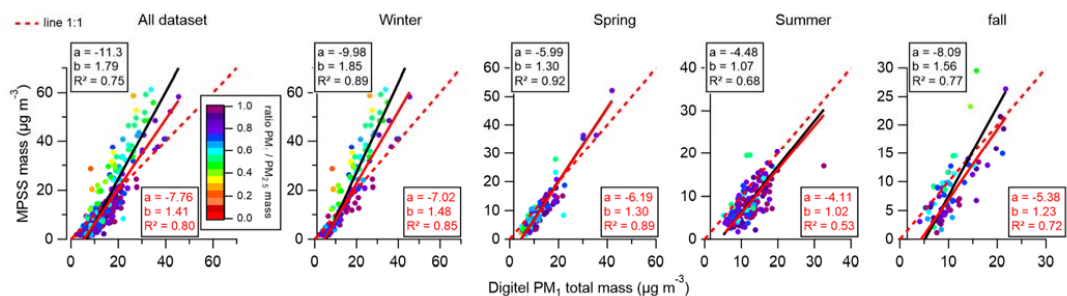


Figure 10: Comparison between filter  $PM_{10}$  total mass concentrations and the MPSS-derived mass concentrations for the entire period (left) and the different seasons. The black lines and boxes correspond to the regression fitting without threshold correction and the red lines to the regression fitting according to a  $PM_{10}:PM_{2.5} > 0.6$ .